DEFENSE DOCUMENTATION CENTER

FOR

SCIENTIFIC AND TECHNICAL INFORMATION

CAMERON STATION, ALEXANDRIA, VIRGINIA

64-11

AFCRL-64-98

DESIGN, DEVELOPMENT, AND CONSTRUCTION
OF MICROMETEORITE DETECTION SYSTEMS

SAMUEL S. CLAPP
Author

RICHARD F. BUCK
Coauthor

FINAL REPORT
December 1963

Contract No. AF 19 (604)-5715
Project 7667
Task 766702

prepared for

AIR FORCE CAMBRIDGE RESEARCH LABORATORIES
OFFICE OF AEROSPACE RESEARCH
UNITED STATES AIR FORCE
BEDFORD, MASSACHUSETTS

**RESEARCH
FOUNDATION**
OKLAHOMA STATE
UNIVERSITY

D D C
APR 14 1964
TISIA

DESIGN, DEVELOPMENT, AND CONSTRUCTION OF

MICROMETEORITE DETECTION SYSTEMS

Samuel S. Clapp
Author

Richard F. Buck
Coauthor

Research Foundation
Oklahoma State University
Stillwater, Oklahoma

Final Report

December 1963

Prepared for

Requests for additional copies by Agencies of the Department of Defense, their contractors, and other Government agencies should be directed to the:

DEFENSE DOCUMENTATION CENTER (DDC)
CAMERON STATION
ALEXANDRIA, VIRGINIA

Department of Defense contractors must be established for DDC services or have their 'need-to-know' certified by the cognizant military agency of their project or contract.

All other persons and organizations should apply to the:

U. S. DEPARTMENT OF COMMERCE
OFFICE OF TECHNICAL SERVICES
WASHINGTON 25, D. C.

ABSTRACT

Contract AF 19(604)-5715, sponsored by the Air Force Cambridge Research Laboratories, has resulted in the design, development, and construction of micrometeorite detection systems to be employed on specific satellite vehicles. A historical background is presented to provide an insight into the study of micrometeorite phenomena and the general theory of the acoustic technique for micrometeorite detection. The objectives of the endeavor are discussed along with the environmental requirements that the systems should withstand. The fundamental design concepts are described categorically; the development of the detection system was the result of combining a suitable sensor assembly, an ultrasensitive amplifier and a digital to analog computer, together with a compatible DC to DC power converter.

The evaluation of the prototype production system is described along with the modifications to the preliminary design, which were incorporated in the production of the micrometeorite detection systems Model D12DN01B.

An engineering revision in the amplifier, discriminator and DC to DC power converter was later proposed and authorization was received to proceed with the production of micrometeorite detection system Model D14DN01. The improvements in the design philosophy are discussed in some detail. Subsequent developments in production requirements and modifications which led to Model D14DN01A-B-C are presented.

The calibration technique employed for the early micrometeorite detection system is compared to a unique "Electronic Striker" which was used for calibration on later models. A comprehensive investigation was made on system sensitivity versus point of impact on a detection plate, and a summary of the analysis is included.

Data from three micrometeorite detection systems, which were flown on the satellite 1961α1, were evaluated. The results are tabulated and compared to previous micrometeorite data. Recommendations are presented which would enhance the validity of the information received from the micrometeorite detection systems on future endeavors.

iii

TABLE OF CONTENTS

TABLE OF CONTENTS (CONTINUED)

LIST OF FIGURES

vii

LIST OF TABLES

1.0 INTRODUCTION

1.1 During the decade prior to the existence of this contract, the effect of micrometeoritic materials impinging on the surface of high altitude rockets had been recognized as a potential problem to the upper atmospheric research vehicles as well as deep space probes and satellites. The fact that meteoritic materials existed in outer space had been known for many years, and toward the end of the eighteenth century the influx of meteoritic materials into the earth's atmosphere had been theorized as the source of the "shooting star" phenomenon.

When the upper atmospheric research program, sponsored by the Air Force Cambridge Research Laboratory was in its infancy, an anomalous indication was recorded at high altitudes on a detection system designed to measure sonic intensities on the surface of the instrumentation package. The mysterious impulses were recorded at random intervals and their occurrence was believed to have been caused by meteoric impacts on the surface of the vehicle. This theory led to a series of instrumentation packages designed to garner information on the relative size and quantity of such meteoritic material.

Several methods have been used to gather information pertaining to the measurements of the influx of meteoric materials. The acoustic method of detection has been employed by the Research Foundation of Oklahoma State University in upper atmospheric research directed toward meteoric influx study. Other measuring techniques have been employed to acquire related data by the flytrap method, as well as by the frangible resistor grid and photodetector systems.

The acoustic method for detection of meteoric particles requires a suitable collecting surface, an ultra-sensitive transducer and an electronics package capable of detecting, sorting, and counting particles. The basic detection system is calibrated in terms of momenta of the particles impinging on the collecting surface. The mass of the particle and the velocity at which it is traveling at the time of impact are individually indeterminate parameters. The total change in momentum of a particle during a finite interval of time is equal to the impulse of the acting force during the same interval and this constitutes the basic theory for the acoustic technique.

1.2 Reports on the following contracts, also with this institution, include details on some early endeavors in the field of micrometeor detecting techniques. The general scope of work overlaps, since the contracts have closely related objectives.

1.2.1 Contract No. AF 19(604)-1908, dated April 1956 to April 1960, "Design and construction of electronic apparatus for amplifying and recording meteoric impacts upon the skin of a high altitude rocket." (Ref. 1)

1.2.2 Contract No. AF 19(604)-7202, dated March 1960 to November 1961, "For research directed toward development of experimental

apparatus for measurement of micrometeorite damage to the surface of space vehicles." (Ref. 2)

1.3   Additional information related to the scientific objectives of this contract can be found in reports on the following contracts with Temple University, Philadelphia, Pennsylvania.

1.3.1   Contract W19-122-ac-12, for research in the physical properties of the upper atmosphere with V-2 rockets.

1.3.2   Contract AF 19(604)-1894, for high-velocity-impact study directed toward the determination of the spatial density, mass, and velocity of micrometeorites at high altitudes.

2.0   PROGRAM OBJECTIVES

2.1   The effective date of this contract was 16 March 1959, and work was initiated 1 June 1959. The original contract was to cover a one-year program, but through a series of extensions with modified Work Statements the termination date was extended to 28 February 1963.

2.2   The original Statement of Work summarized the contract objectives as follows:

"The Contractor shall supply the necessary personnel, facilities, services and materials to accomplish the following:

Item 1 - Design, develop and construct meteoritic microphone detectors of various sensitivities for use in satellites. The microphone detectors shall have a sensitivity in the neighborhood of 10^{-4} gram-centimeters per second (impact on a 1/16" steel plate).

Due to the nature of the contract, several closely related phases of activity were performed during the time interval for which the contract was in existence. These phases will be handled in a chronological sequence which will include pertinent information and describe techniques employed to accomplish the design, development, and construction of the micrometeorite detectors.

2.3   The micrometeor detecting systems developed under this contract were to be incorporated in the instrumentation section of a vehicle provided by the Lockheed Aircraft Corporation. Details affecting both the electrical and mechanical design criteria were outlined in the general environmental specifications for the vehicle, and were published as Lockheed's Specification LMSD-6117A, dated 24 June 1959. The thermal environment was established as encompassing a temperature range bounded by -30° Centigrade and +85° Centigrade. The mechanical criteria include the following requirements as set forth by LMSD-6117A:

2.3.1   When packaged for shipment, the system shall be capable of withstanding drops to a flat concrete surface in both directions along each of the three major mutually perpendicular axes

2

and each of the principal diagonal axes from a height of 42 inches.

2.3.2 The assembled system shall be capable or withstanding vibration at a frequency and amplitude of 3000 cps and 20 g, respectively.

2.3.3 The assembled system shall be capable of withstanding an approximately half-sine shock wave with a duration of six milliseconds and a peak amplitude of 40 g's.

2.4 The above environmental requirements essentially cover the anticipated limits during ascent of the vehicle. Once in orbit, these requirements are considerably reduced such that the thermal limits become -30° C to $+60^\circ$ C, and the mechanical stresses approach zero. However, once in orbit the equipment shall be subjected to other environmental stresses. The more significant of these are pressure (vacuum), particle bombardments, and energy radiations.

2.4.1 The anticipated pressure was 10^{-8} to 10^{-9} mm Hg.

2.4.2 Several penetrations of the vehicle skin by meteorites per year may be expected. Erosion due to micrometeorites should be negligible for 90-day operation. These effects may be considerably increased if meteoritic showers are encountered.

2.4.3 Primary cosmic radiation, that is, the incidence of high velocity nuclei of elements, was anticipated. Because of their extreme velocities, these particles are very penetrative, and leave an ionized trail through the material, but cause little overall damage due to the low particle flux. Because of the high velocities, shielding weight was prohibitive.

2.4.4 At high altitudes there is an intense low energy radiation made up of charged particles trapped in the earth's magnetic field. Its altitude at low latitudes has been reported as above 600 miles. There is reason to believe that the radiation will be encountered at lower altitudes in polar regions. At the present time, sufficient information on the energy distribution of this radiation is not available for use in design considerations.

2.4.5 Albedo cosmic rays are secondary cosmic radiation caused by primary cosmic radiation striking the earth's atmosphere and disintegrating the target nuclei into smaller, lower energy particles. The portion of the secondary radiation which is radiated to space is referred to as Albedo cosmic rays. These rays will cause molecular sputtering of the skin and damage to components mounted at the surface. Damage produced is unknown but is expected to be slight for 30-day operation.

2.4.6 Ultra-violet, extreme ultra-violet, and X-ray radiation produce damage to non-metallic materials by breaking down the chemical bonds. Thin metallic foils can be employed to shield these materials. This radiation might produce a slight static charge on the vehicle due to photoelectric effect. However, this charge is probably counceracted by other effects.

3

3.0 FUNDAMENTAL DESIGN CONSIDERATIONS

3.1 Scientific Report No. 1 on Contract AF 19(604)-5715 (Ref. 6) describes the original design of the micrometeorite detection system. This system was designated as D12DN01B and will be referred to as such throughout this report. The design techniques employed in the DC to DC converter and the logic section were given particular emphasis in this report. Although a portion of the subsequent material will be of a repetitive nature, it is considered essential to the coherency of this report.

3.2 The Model D12DN01B micrometeorite detection system can be broken down into four basic sections which are the sensor assembly, the high gain amplifier, the logic section, and the power supply. The individual systems and their relative functions will be discussed along with the mechanical packaging philosophy and the data output from the system. The design of the logic section and the power supply will be summarized, since it has been submitted previously and an improved design of basically the same circuit is included in Appendix I of this report.

3.2.1 Acoustic Sensor Assembly. A micrometeorite sensing system employing the acoustic technique had been used in conjunction with a miniature counting unit which was developed, by this institution, under Contract AF 19(604)-1908 (Ref. 1). The acoustic technique requires a meteorite collecting surface and a very sensitive transducer to convert the minute mechanical stimulus, which was created by impinging meteoritic materials, into an electrical output signal. The Statement of Work for this contract specified that the transducers would be microphonic and that the collecting surface would be constructed of 1/16-inch steel plate. Additional factors which influenced the final design were the anticipated mechanical vibration and the necessity for acoustic isolation between the collecting mechanism and the main structure of the vehicle. Acoustic isolation was predicated by the basic theory of the detection system in that any mechanical disturbance to the collecting surface would be detected by the microphone and produce electrical signals which would be interpreted as meteoritic impacts. The collecting plate, which had been used on previous experiments, and its associated mounting arrangement would not meet the mechanical vibration specifications set up for this system.

Two interrelated functions had to be given careful consideration during the design of the sensor assembly. The design criteria had to be such that the unit would meet the mechanical vibration specifications, and it had to be constructed so that the detecting characteristics of the collecting plate remained as high as possible. The number of support points, the method of suspension, and the location of support points were eventually chosen as a compromise between achieving the requisite sensitivity and still maintaining the desired structural rigidity for the final assembly. Two stiffening creases were made in the plate in an attempt to break up the vibrational modes on the plate. The collecting plate was supported at eight points by silicone rubber grommets which were compressed to a predetermined level

4

by screws through a metal insert. The mechanical structure for the sensor
assembly is shown in Figure 1, (OSU drawing C12DMO1B).

Figure 1.   Assembly, Micrometeorite Sensor

The microphone for the sensor assembly was developed by
Temple University, Philadelphia, Pennsylvania. It was a supersonic
piezoelectric device designed for a resonant frequency in the neighbor-
hood of 100 kilocycles. When the microphone received a mechanical
stimulus, it produced an electrical signal proportional to the amplitude
of the mechanical forces acting on it. The magnitude of the 100 kilocycle
signal output from the microphone was very low and its anticipated maxi-
mum output, for the low energy level impacts, was less than twenty micro-
volts.

Early experimentation with the microphone type detection
system used an epoxy bond (Emerson and Cuming, Eccobond 56C) between
microphone face and the rear surface of the sensing plate. This feature
was later eliminated because variations in system sensor sensitivity
were found attributable to variations in the potting technique and aging
effects. A short investigation of optimum mounting methods disclosed

5

Figure 2. Micrometeorite Sensor Assembly

6

that more uniform characteristics could be obtained if a small dimple
was made in the surface of the sensor plate, so located as to bear
against a single point on the face of the microphone. These same studies
also disclosed there was an optimum force with which the microphone
should bear against this dimple for each individual microphone. (Ref. 2)
A special three-legged bracket was used to hold the microphone in posi-
tion, with the mounting points adjusted to achieve the desired force for
each individual microphone. In the final version, an epoxy bond around
the microphone dimple contact was used to prevent the microphone shifting
position after installation at the desired force level.

This configuration proved to be the most practical
since it provided the required mechanical characteristics while applying
minimum constraint to the microphone. For optimum acoustical properties
of the sensor assembly, it was desirable to have a minimum number of
support points and to reduce the microphone restraint. Restraint
effectively lowers the Q of the piezoelectric crystal and this results
in lower system sensitivity. Both the triple support of the micro-
phone and the eight-point support of the plate had an adverse effect on
the system sensitivity. However, sensitivit'es of the order of 0.3 to
0.6 X 10^{-3} gm cm/sec were still possible. The micrometeorite sensor
assembly is shown in Figure 2.

3.2.2 Amplifier. The microphone output was transferred to
the input of the amplifier via a coaxial cable. The amplifier was a
high gain, stagger-tuned unit with a passband of ten kilocycles at
approximately 100 kilocycles. It was possible to shift the amplifier
passband so that it amplified the maximum output response of the par-
ticular microphone which was selected for each individual system. It
was impossible to avoid this selection since the individual microphones
varied in sensitivity and frequency response. The microphone amplifier
matching could have been ignored only at the expense of overall system
sensitivity.

Work was initiated on this project in June 1959, and the
prototype system was scheduled for final acceptance tests in the early
fall. Due to the accelerated work schedule requirements, a decision
was made to repackage the amplifier section of the micrometeorite de-
tection item which had been developed under Contract AF 19(604)-1908.
(Ref 1) A schematic diagram is shown in Figure 3. This amplifier did
not possess the optimum characteristics, but it had been proven as an
adequate design in previous experiments. A revised amplifier was to
be developed and incorporated in the detector package after the pre-
liminary requirements for the contract had been fulfilled.

The amplifier section was basically a three-stage
stagger-tuned configuration. Type 2N147 transistors were used for this
portion. Some degree of gain- and bias-stabilization is achieved through
the use of emitter resistors adequately by-passed for signal frequency
on all three stages. In addition, a small amount of degenerative feed-
back is provided from collector to base on the input and output stages;
the second stage is operated at maximum gain with no feedback. The
first two stages are operated at a reduced collector supply potential

7

Figure 3. Amplifier Circuit D12DN01B System

set by R206, a series dropping resistor adequately decoupled by C201.
The transformers used for T201 and T202 have a fairly poor coefficient
of coupling and give an effective impedance transformation ratio of
approximately six to one by virtue of this loose coupling. Details of
the transformer design are given in Figure 4; the 400 series code
numbers on this OSU drawing A10RQ13A-B corresponds to the 200 series
in the amplifier schematic Figure 3. The output winding feeding the
base of the following stage is carried at the DC potential of the base
and is by-passed, not to ground, but to the emitter for the stage in
question. Since the first two stages operate at extremely low signal
levels, no compensation in base bias is employed. However, some degree
of base-bias compensation is provided for the third stage by the base-
bias network of R207 and R208, in series to the collector supply poten-
tial. Amplifier response is controlled by choosing the proper values
for C202, C207, and C210 in order to tune each stage to the desired
frequency. In general, the first and second stages are tuned to the
low side of the passband, and the output stage (which operated into a
simple resonant circuit) is tuned to the high side. Some control of the
effective in-circuit Q of the third stage is afforded by resistor R209,
whose value is selected for each individual unit to provide optimum
amplifier response. The ratio of output voltage at the collector of the
third stage to input voltage at the base of the first stage indicated a
relative gain of approximately 105 decibels with this design. (Note that

8

this is not power gain but the voltage ratio from input to output; the impedance of the output stage has not been taken into account in quoting this figure.) In order to achieve this gain figure for the simple three-transistor configuration involved, it was necessary to select the transistors which were used for the amplifier portion. All transistors procured for this contract were individually tested on a Tektronix Type 575 Curve Tracer, and only those units showing beta values of approximately 40 were selected for use in this service; those transistors which indicated a "soft knee" in the characteristic family were not used.
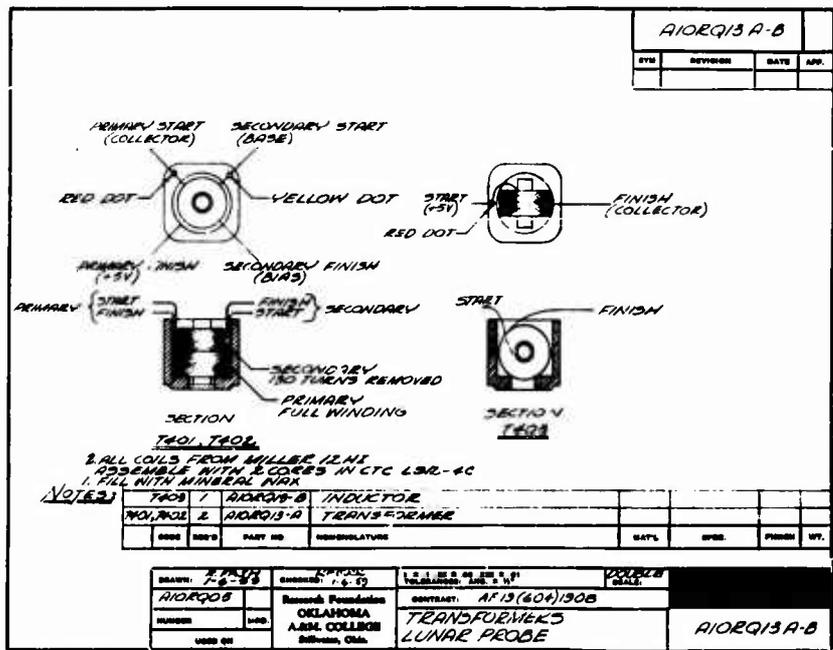
Figure 4. Transformer Design for D12DN01B Amplifier Circuit

3.2.3 Logic Section. The input to the logic section is the output signal from the sensor assembly—amplifier combination. The magnitude of the amplifier response represents a linear function of the momentum of the incident particle at the point of impact on the detecting plate. The impact signal is amplified and read out on two lines; either the "A" line alone, indicating a small momentum impact, or both the "A" and "B" lines, indicating a large momentum impact. An "A" impact was defined as any impact which caused an input signal to appear on the input line to the "A" register, with an arbitrarily selected negative

9

peak amplitude as a maximum limit. A "B" impact was any impact causing
an input signal with a peak amplitude exceeding the arbitrary maximum
limit chosen for the "A" signal. The "A" line and "B" line are connected
to the "A" and "B" registers respectively. An "A" or "B" impulse on
the respective line causes that register to be advanced one position.
The "A" register has a capacity of eight impacts prior to recycling, and
the "B" register has a capacity of only two impacts, where upon it will
recycle.

Even though the total storage capacity for the "A"
register was eight events, the early versions of this equipment were so
arranged to read only every other "A" event, leaving an "unread"
ambiguity for a continuous length of record. The total number of "A"
events could be determined with an accuracy of plus or minus one event
for any continuous sequence of data by merely doubling the number of
"A" shifts involved and adding one to correct for an unread event,
which could occur at the beginning or end of each sequence. (Ref. 3)
The choice of this philosophy was dictated by the assumed availability
of only eight discrete levels within the telemetry band. Since the
"B" register would divide these eight events into two groups of four,
it was necessary to restrict the "A" readout. Later versions of the
equipment were arranged so as to permit an optional 16 level output
signal by adding the level from the first "A" register to the two
normally connected to the mixer input line.

The outputs of the "A" and "B" register were connected
to the A-B mixer. Here they were converted from multiple two level DC
signals to a DC analog output having eight discrete voltage levels.
Each discrete output level on the A-B mixer indicates the unique com-
bination of states of the A and B registers. (i.e. either one B and
two A's or one B and four A's or one B, 6 A's etc.) Figure 5 depicts
a block diagram showing the prototype system exclusive of the power
supply section.

The output signal was restricted to positive values
only with respect to a reference voltage common to both the system and
the telemetry. The peak amplitude of the output signal was specified
as equal to or less than five volts. Final recorded data was estimated
as resolvable to ± 2 per cent of full scale; the absolute accuracy was
estimated as ± 5 per cent of a full scale. Using the full scale range
of five volts, this would indicate the minimum detectable step would be
in the order of ± .1 volts during real time readout. The absolute
accuracy estimate required the nominal voltage levels, used to represent
information, to be at least 0.25 volts apart. This minimum voltage
level of separation predicated the maximum number of voltage steps
available to represent information. The quality control of commercially
available components and the inherent voltage drift of semiconductor
products when submitted to wide temperature ranges were considered,
and a choice of 0.6 volts per output step was selected as a reasonable
level. With a five-volt maximum output, eight discrete levels would be
available to represent data reliably for transmission to monitoring
stations.

10
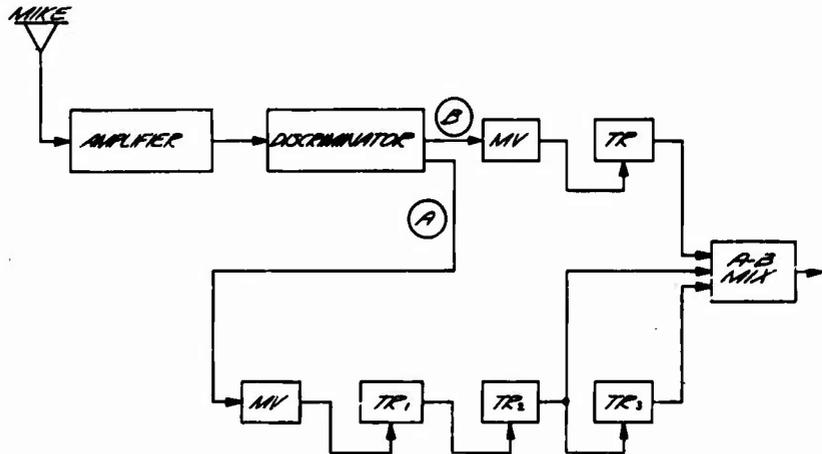
Figure 5. Block Diagram of Micrometeorite Detection System

3.2.4 Power Supply. Preliminary specifications for the power supply called for both ac and dc isolation of the signal ground and power ground. This requirement prohibited the use of a simple resistor-zener diode regulating device and made a DC to DC power converter imperative. A two transistor oscillator and a small power transformer was designed for this purpose. Filtering, rectifying, and regulation was provided at the output of the transformer. The transformer provides the isolation between power ground and signal ground. The voltage input to the DC to DC transverter was 28 volts, and the outputs were ± 6.8 volts and ± 5 volts. The ± 6.8 volt levels were obtained by using a zener diode regulator. The ± 5 volt supplies were obtained by using suitable resistors and voltage dividing the ± 6.8 volts to ground.

3.2.5 Internal Temperature Sensor. At the outset of the development activity, a request was made that a suitable sensor be incorporated within the instrumentation to permit measurements of the actual ambient temperature within the final electronics package while under orbital conditions. Discussions with personnel of Lockheed

11

Missile Systems Division (LMSD) disclosed that a temperature bridge
arrangement was already scheduled to be incorporated in the vehicle in
which the system was to be installed. It was agreed that an identical
sensor would be incorporated within the D12DN01B system, and suitable
external switching would connect this into the standard bridge on a
time-sharing basis with other temperature gages of this same charac-
teristic. Accordingly, the RDF Stikon Model BN-1200 temperature gage
manufactured by Ruge Associates was selected for this application in
order to establish compatibility with other identical external gages
aboard the same vehicle. This device was of the platinum wire, re-
sistance thermometer type. It was incorporated within the mixer
module because environmental testing had disclosed that this portion
of the circuitry was the most critically temperature dependent part of
the system. In the event ambient temperature exceeded the design
specifications, ambiguous levels could be achieved from the mixer be-
cause of temperature-dependent variations in the base current of the
transistor used in the mixer circuit. Inclusion of the temperature
sensing device in this circuit permitted preflight calibration and
post-flight correction for extreme temperature levels, in the event
such conditions existed in flight. The gage was connected from the
center terminal of P101-4 to the system ground within the unit.

3.2.6 Mechanical Design. Several different packaging
techniques were investigated for the micrometeorite detection system's
electronics. The systems were to be incorporated on a specified Lockheed
vehicle and a practical mechanical design which would facilitate in-
stallation was considered important. Although a compact system was
desired, the size and weight of the package were not extremely critical
parameters. The physical size and configuration of the final product
depended on the method selected for assembling the electronic circuitry,
which would be contained in the package.

The design and development of early micrometeorite
detection systems, by this institution under Contract AF 19(604)-1903,
(Ref. 1) provided an insight to the potential difficulties which could
be encountered. These early systems had been constructed to produce
a maximum packing factor. The overall results were satisfactory, but
from the repair and modification viewpoint, the maximum packing factor
concept was not desirable. Regardless of the effort expended in the
design and development of an electronic system that will function properly
over wide temperature ranges, all transistors of a specified type will
not perform with the desired efficiency in any given circuit. The com-
ponents were submitted to various acceptance tests prior to installation
but from experience it has been found that all potentially undesirable
characteristics cannot be detected during simulated circuit testing.
With this knowledge as a basis for future packaging, the building block
philosophy of internal construction for the detector systems electronics
was selected as the most desirable, as will be substantiated later.

The required circuitry for the micrometeorite detection
system was studied and tentative circuit layouts indicated that all cir-
cuits could be adapted to an etched circuit board which was 1 1/8 by 1 1/4
inches. The basic plan was to construct independent circuits for the
logic section bistable and monostable multivibrators onto one of these

12

Figure 6. Assembly, D12DN01B Detector System Electronics Package

printed circuit boards, and to divide the amplifier and power supply
section into subsections. The amplifier was a three-stage stagger-tuned
system and each stage could be conveniently installed on a standard size
printed circuit card. The DC to DC power converter was also adaptable
to this philosophy on three standard size cards which incorporated cir-
cuitry for the oscillator, transformer and rectifier-regulator on in-
dividual boards.

The building block philosophy of internal packaging
has several advantages. Each subsystem could be tested individually
prior to installation into the package. If the system indicated abnormal
operating characteristics, the problem could be isolated in a module.
The faulty module could be removed and repaired, or it could be replaced
by a spare module depending on the nature of the malfunction and the
time available to accomplish the repair.

The electronic components were mounted to the printed
circuit board and the required interconnection leads were attached to the

13

Figure 7. Electronics Package for Detection System Dl2DN01B

proper points. A maximum of eight interconnecting leads on one-eighth inch spacing could be extended from a card. The finished card was placed in a machined mold with the interconnecting leads protruding through clearance holes in a predetermined order. Emerson and Cuming Inc. Eccofoam FP compound was used to encapsulate the printed circuit board. The finished product was a module which measured 1 1/8 by 1 1/4 by 11/16 inches, with the necessary interconnecting leads protruding in a straight line from one edge.

Fourteen modules were required to accommodate the subcircuits in the detection system. The modules were attached to a master etched circuit board, which had been laid out to provide a maximum of eight lead positions for each module. The interconnecting leads from the modules were inserted through the master board and soldered to the etched circuit side of the board. The master etched circuit board was 1.4 inches wide and 7.87 inches long. The assembly of the micrometeorite detection system can be seen in Figures 6 and 7.

Five Microdot connectors No. 31-01 were installed on the end of the package to accommodate signal input, power requirements, and data output. The connectors were wired to the proper points on the master etched circuit board. The connector end of the electronics package was divided into appropriate areas around each Microdot connector and color coded according to a mutual agreement with Lockheed personnel.

4.0 MICROMETEORITE DETECTION SYSTEMS - D12DN01B

4.1 The prototype production model, Serial No. 1, for this series was completed. After partial environmental testing, it was delivered to AFCRL headquarters for additional testing on 20 October 1959. Since this unit was the prototype, its operation was studied rather closely so that any undesirable characteristics could be detected and then be corrected on the subsequent systems. As could be expected, a few undesirable features became evident as the evaluation progressed. The unit was not modified to incorporate any design revision, but it was regarded as a sufficiently close prototype to permit preliminary familiarization and evaluation by AFCRL. By mutual agreement, this prototype unit was to be returned to OSU for updating, reworking, and final acceptance testing.

The prototype unit was submitted to more than 1000 hours of operation during the tests and evaluation prescribed in the Lockheed Specifications LMSD-6117A, which are summarized in Section 2.3 of this report. Once the initial problems had been worked out of the system, it functioned satisfactorily until it experienced a catastrophic failure of a sensistor in the power supply section during a 100 g load shock test performed by AFCRL. The cause of this failure was traced to the method by which the sensistor was mounted within the unit. Oklahoma State University Research Foundation did not have facilities to perform the very high g load shock tests; consequently, the problem was not discovered until such tests were conducted. The installation of this sensistor was corrected to eliminate the possibility of a second failure.

15

4.2 During the evaluation tests, a few marginal design features became apparent. The circuits had been designed using passive elements with ± 10 per cent tolerance and germanium transistors. Although the worst case philosophy had been used for the design, the temperature range set-up for satisfactory operation was somewhat rigorous for germanium semiconductor characteristics. Typical examples of the required modifications on individual portions of the circuit, to establish compliance with the environmental test specifications, follows:

4.2.1 The first and most significant deviation from the desired operating characteristic was detected as a shift in the output levels from the power supply which were required for proper operation of the associated equipment. The initial design of the DC to DC power converter had ± 6.0 volt outputs as the prime supply, with tapped outputs at ± 5.0 volts. Environmental testing of the unit revealed that the potential difference between the 5.0 volt bus and the 6.0 volt bus did not provide an adequate margin of safety, for the biasing technique employed in the logic circuitry under thermal conditions. The transformer design was modified to permit the ± 6.0 volt output level to be increased to ± 6.8 volts for the prime supply. Two benefits were achieved here: first, the availability of the slightly higher operating voltage resulted in a slight increase in gain for this system. Second, zener diodes regulating at 6.8 volts were available with characteristics sufficiently better than those available at the original output of 6.0 volts. The improved zeners would automatically improve the regulation of the power supply section. At the same time these changes were made, thermal difficulties resulting in the loss of regulation of the ± 5.0 volt supplies was evaluated and found to be due to insufficient base bias current into the regulating transistors. Revision of the circuit, by replacing these transistors with 5.0 volt zener diodes, improved the stability markedly in this portion of the equipment. While this modification was being accomplished, an undesirable ripple was noted. The residual ripple component on the output buses was due to the audio frequency component arising from the fundamental oscillator frequency. Addition of capacitor filters on all output buses reduced this to a tolerable level.

4.2.2 The single shot multivibrators which are used as pulse standardizing circuits between the amplitude discriminator and the binary storage registers were also modified. Originally both the collectors had been returned to ground and the emitters operated from the - 5.0 volt source. By returning one collector the + 6.8 volt line, the temperature stability of the single shot was improved tremendously. At the same time this change was made, the multivibrator time constant was also modified slightly. The cross coupling network from the normally "on" transistor to the "off" transistor was modified for greater reliability under conditions of low temperature operations.

4.2.3 The cross-coupling networks in the binary circuits were modified similar to that described for the single-shot multivibrators to improve thermal stability in these units. The tap point provided on the output collector of each binary was modified so as to provide increased drive to the following binary registers. The new voltage level,

16
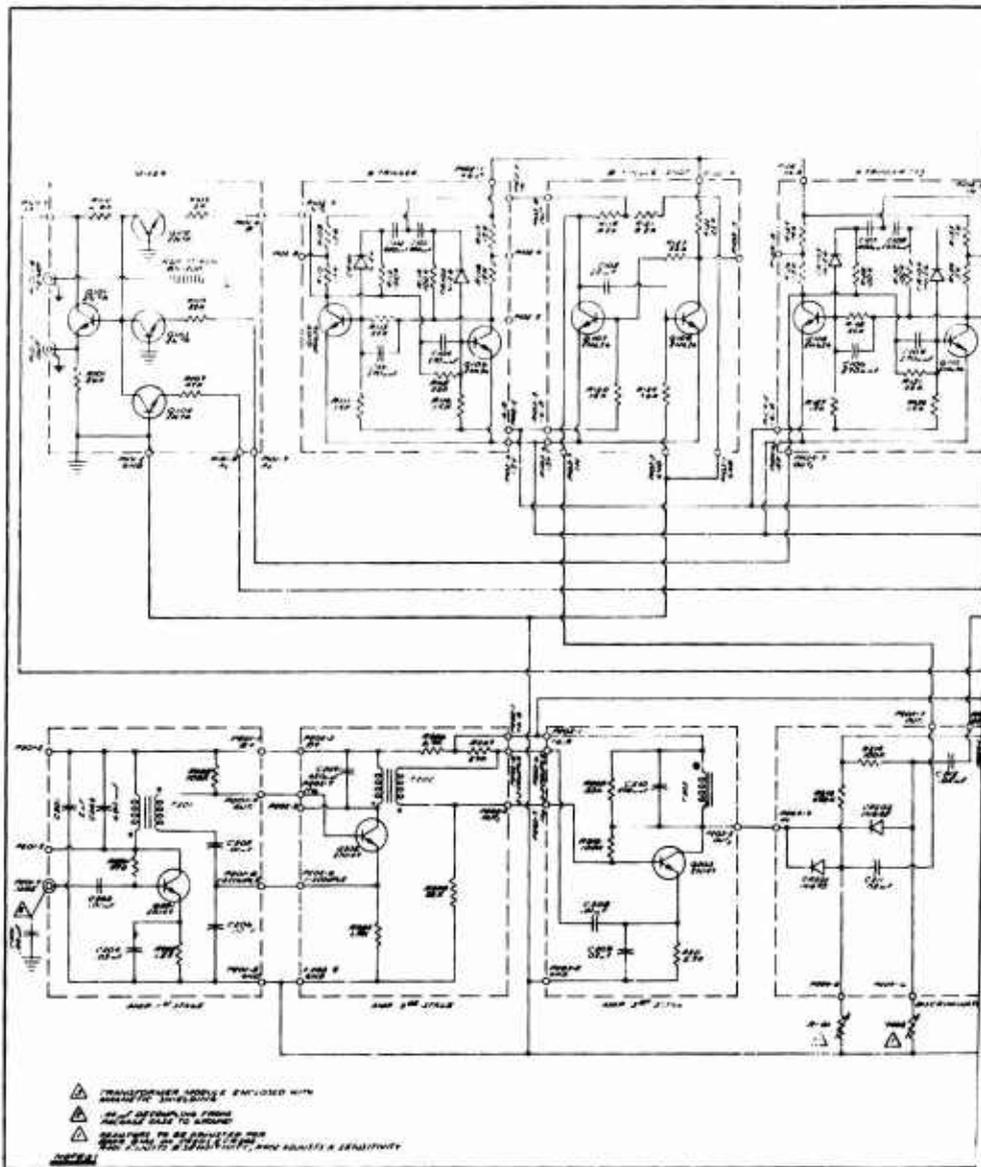
Figure 8. Schematic, D12DN01B Detector System Electronics Package

17

6.8 volts, from the power supply in lieu of the original six-volt power supply improved the stability and reliability of the binary register circuit.

4.3 After the prototype model had been submitted to the specified environmental testing and the modification described in Section 4.2 had been incorporated into the design, a total of twelve Model D12DN01B units were constructed according to OSU drawing D12DN01B, Figure 8, and designated as serial numbers 1 through 12. These units were delivered to AFCRL as they were completed. Their calibrated sensitivity was recorded and it is presented in chronological order in Table 1 (Page 32).

4.4 The maintenance performed on the prototype system, Serial No. 1 of Model D12DN01B, was explained in detail earlier in this section. It should be pointed out that a new power supply was installed which increased the B^+ level from the original 6.0 volts to 6.8 volts. The amplifier had been tuned using the 6.0 volt source, but it performed very well when the supply voltage had been increased. The revised logic system was also installed in this system prior to final checkouts and acceptance tests. The second calibration for this system, which is shown in Table 1, was taken after the updating had been completed.

Serial No. 2 was returned to OSU for repair in April 1960 with a trivial malfunction. The problem had presented itself as an intermittent output from the logic section. Teflon tape, Temp-R-Tape T, had been used to secure the output leads to the master printed circuit card to prevent them from flexing during high frequency shake tests and during flight. The adhesive on the tape had collected some foreign matter and was effectively shorting out the logic output on occasions. The system performed satisfactorily after the tape had been removed, and it was recalibrated prior to returning it to AFCRL.

A reduction in the sensitivity level was noted during checkouts by Lockheed personnel on Serial No. 3. These reports were confirmed by AFCRL, and the system was returned for repair 16 February 1961. The difficulty was traced to a "cold" solder joint on the "A" monostable multivibrator. At this time, the new version of the micrometeorite detection system, Model D14DN01A, was in production, and the discriminator and both monostable multivibrators were replaced by their counterparts from the improved system. The A_1 and A_2 triggers were modified to give an advance pulse of approximately five volts. The system was recalibrated and given the Serial No. 3A, since it was now a hybrid version.

At Lockheed, Serial No. 11 was accidentally left connected during a high potential check on the vehicle and it was severely damaged. This system was returned for repair 14 February 1961. The amplifier section was the only part that escaped damage. Here again the modules from the D14DN01A system were installed in place of the damaged subassemblies. The conversion was not simple for the power supply, and several jumper connections were required to achieve the desired results. Since a major portion of this system was comprised of the D14DN01A electronics, it was assigned Serial No. 11A for identification.

19

Serial Numbers 2, 9, and 12 were returned along with several of the later systems in 1962 for general evaluation and repair if necessary. They were all in operating condition, but S/N 12 had been damaged physically. The sensor plates were not returned for Serial Numbers 2 and 9 so an approximate sensitivity check was made using Sensor Assembly No. 12. The sensitivity calibrations are recorded in Section 2 of Table 1 (Page 32)..

5.0 REVISED MICROMETEORITE DETECTOR SYSTEM - D14DN01

5.1 The immediate obligation to the subject Contract AF 19(604)-5715 had been fulfilled when the twelve systems of Model D12DN01B were delivered to AFCRL. It was pointed out in Section 3.2.2 of this report that the original amplifier design would later be improved and incorporated into the micrometeorite detection system. Although preliminary study of a proposed system had been pursued for several months, the actual production of the D12DN01B systems had been of primary importance and the revised amplifier prototype had been underway as a secondary project. Experience gained during the design and production of the previous units instilled a desire to improve the power supply and also to make minor modifications to the logic section. Since these alterations, coupled with the improved amplifier, essentially created a new concept for the detection system, an Interim Engineering Report on the proposed system D14DN01 was submitted in May 1960 to AFCRL and approved by this agency. (Ref. 4)

The subject contract assumed a new perspective when the proposed system Model D14DN01 was approved. All work performed on this Contract AF 19(604)-5715 would be directed toward construction of "flight model" hardware and the required effort to finalize the electrical design of the proposed Model D14DN01 micrometeorite detection system would be conducted under a sister contract, Contract AF 19(604)-7202.

5.1.1 A master's thesis by Dave C. Mueller entitled "A Transistorized Digital Computer with Both Real and Stored Time Analog Readout of Information - for Use in Deep Space Investigations of Micrometeor Phenomena" included in this report as Appendix I, describes the logic section and the power supply design, as well as the environmental testing procedure and packaging techniques employed on the D14DN01 systems. This thesis was submitted to the faculty of the Graduate School of the Oklahoma State University in partial fulfillment of the requirements for the degree of Master of Science, Electrical Engineering, in August 1960.

5.1.2 The amplifier for the D14DN01 system provided the major portion of the circuit gain through the use of the two tuned stages at the input. Unilateralization was used on these two stages, since it was impossible to design an inherently stable high frequency amplifier using transistors without including this feature. The second stage was followed by an emitter-follower which provides isolation between the two high-gain tuned stages and a final common emitter output stage. This output stage was designed to provide sufficient gain to drive the associated discriminator section of the acoustic detection system. The amplifier circuit is shown in Figure 9. The design of

20
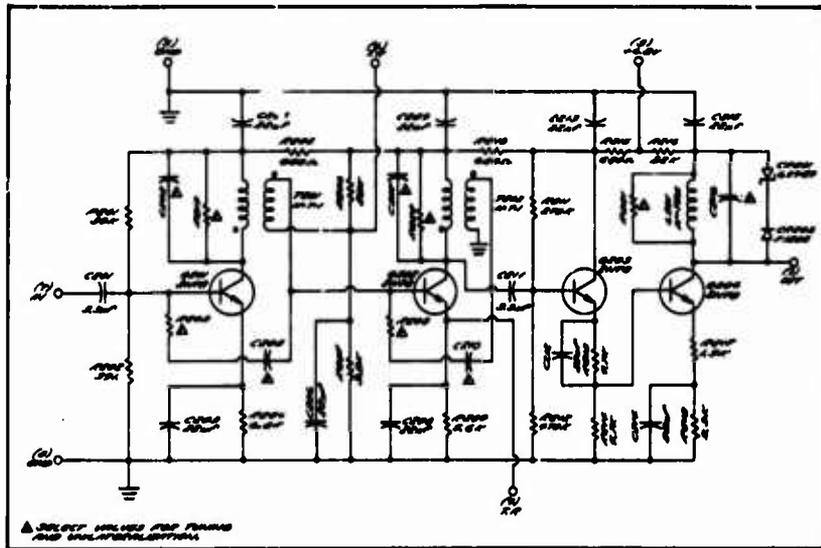
Figure 9. Revised Amplifier Circuit D14DN01 System

the system was conducted under Contract AF 19(604)-7202 and a detailed functional analysis was presented in the final report for that contract. (Ref. 2)

5.1.3 The building block concept of modular assembly was retained for the electronic subassemblies, but experience gained during the testing and evaluation of the D12DN01B systems proved that the amplifier and power supply submodules were functionally inseparable. For example, if any one of the amplifier stages became faulty, it was necessary to remove all three of the individual amplifier modules to work on the amplifier bandpass. Since the stages were stagger tuned, a direct substitution of a duplicate unit would not be feasible, because the individual stage tuning is naturally a function of the input impedance to the second stage. Although the parameters can be calculated and obtained within ten per cent, a ten kilocycle bandpass at 100 kilocycles cannot be achieved satisfactorily with a random selection of subassemblies. Therefore, the revised amplifier was constructed on a single etched circuit card having nominal dimensions equivalent to three of the smaller standard sized cards used elsewhere throughout the system. Similarly, the power supply was constructed on a single larger card. These two enlarged cards were encapsulated by the same method used for the standard modules and incorporated into the system as shown in Figure 10. The amplifier had required four of the standard individual modules in system D12DN01B, and the power supply had required three standard modules. The

21
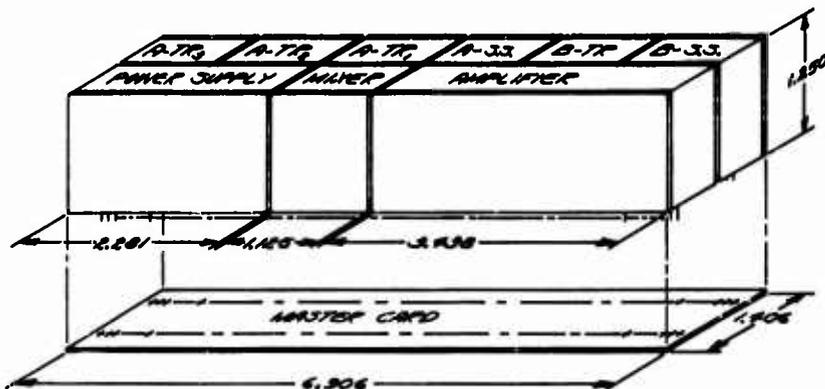
Figure 10. Module Display D14DN01 System

revised concept eliminated two standard modules and an overall reduction of approximately 1 1/8 inches in the length of the Model D14DN01 package was achieved. The pattern for the six external mounting holes used for affixing the package to the flight vehicle was not changed.

     5.1.4 A revision to the mechanical package was proposed by AFCRL to facilitate installation of the system in test rigs during pre-flight evaluation, and on the Lockheed flight vehicle. Four of the Micro-dot connectors, used for electrical interconnections on the D12DN01B units, would be replaced with a multiple pin connector. A Bendix connector, Part No. PTO2A-14-15P, was selected as being the most desirable. The connector is keyed and this feature eliminates the possibility of making erroneous connections. The single Microdot connector retained on the mechanical package is for connecting the microphone cable from the sensor assembly into the amplifier of the electronics package.

    5.2 The coordination required for Lockheed to incorporate the new electrical interconnection system into their vehicle had not been finalized when delivery of four detection systems was requested by AFCRL. The prototype D14DN01 micrometeorite detection system had been submitted to the prescribed environmental tests. The amplifier gain and stability indicated a considerable improvement over its predecessor, and the new power supply operated very well. Based on the results obtained during the environmental test on the prototype system, the production request could be fulfilled using the new electronics system equipped with the five Microdot connectors so that compatibility could be retained with

22

the current Lockheed facilities. This actually created an intermediate system whose existence had not been anticipated. Therefore, these systems (Serial Numbers 13, 14, 15, and 16) assumed the designation Part No. D14DN01.

The prototype system was reproduced in quadruplicate, and two of the units were calibrated and delivered to AFCRL. The anticipated launch schedule permitted further evaluation of the two remaining production models. The major endeavor, during these evaluation tests, was to evaluate the reproduction effort required for the amplifier. It was acknowledged that the transistors for the two tuned stages would have to be selected to achieve the desired gain and unilateralization characteristics. Aside from this unavoidable selection, the design objective had been to develop a system that was straight forward for reproduction purposes. The tests on these first four duplicates of the prototype system indicated that special techniques and precautions would be necessary if the present design was used in further production. The difficulty apparently was isolated to the output stage of the amplifier. A new toroid was installed in the collector of this stage and it was tuned for a broad bandpass, which would effectively amplify the output from the preceding tuned stages. This alteration was made on the two remaining systems with improved results and thus permitted delivery and the required quantity of four interim systems, while development continued on a revision of the output stage circuitry.

5.3 The original output stage of the prototype D14 series amplifier had been designed with a unique reactive load arrangement in the collector circuit. In order to minimize the system response to amplifier noise, which has the majority of its power concentrated in frequencies significantly higher than those passed by the earlier stages of the amplifier, it was desirable to have a capacitive load for the fourth stage. As the frequency of the noise component increased, the collector circuit impedance would decrease and thus reduce the voltage gain of the stage. A toroidal coil with self-resonance in the neighborhood of 30 kilocycles was used on the prototype system to gain the characteristics described above. This amplifier had functioned quite satisfactorily and did achieve the desired reduction in noise. However, sensitivity checks taken after improving DC stability (through modification of the bias networks) revealed that the overall sensitivity of the amplifier was not consistent with the desired level for the system when using the capacitive output circuit. The output coils were tuning at approximately 50 kilocycles (approximately one-half the center frequency for the amplifier passband) when placed in the circuit. Some difficulties in stability were also noted for coils whose true resonance was thus placed in a "subharmonic" relationship to the final output frequency. In order to improve both gain and stability, the coil of the last stage was designed so that its self-resonant frequency was well above the operating frequency of the amplifier and this stage was tuned to amplifier center frequency by adding parallel capacitance. The "Q" was controlled by a parallel resistor, loading the circuit to such a value as to prevent end-to-end feedback and consequent oscillation. (Ref. 2) Beginning with Serial No. 17, all subsequent micrometeorite detection systems incorporated this revised amplifier design and the series assumed the designation Part No. D14DN01A.

23

5.4 In normal D14DN01A systems, identical modules were used for both "A" and "B" monostable multivibrator discriminators. Because of the reduced voltage shift available at the triggering point of the multivibrator due to the steady-state bias required for discrimination on the triggering transistor, the total timing action was somewhat reduced on the "B" multivibrator with respect to the "A" multivibrator. This permitted recovery of the "B" discriminator slightly ahead of the "A" discriminator in the case of detection of very large events. This was originally felt to be a desirable feature in that it seemed to decrease the chance of spurious "A" triggers being generated upon recovery of the "B" monostable multivibrator from the stimulus provided by a large momentum event. However, later experience indicated that optimum reliability could be achieved with both "A" and "B" discriminator sections recovering together. As a result, the timing circuit was modified in the "B" multivibrators in order that "A" and "B" multivibrators might recover simultaneously. (Ref. 2) This design change, coupled with another minor change which increased the output drive from the binary circuits was incorporated in the subsequent systems starting with Serial No. 21 and designated as Part No. D14DN01B.

A total on nine detection systems, Serial Numbers 21 through 29, were constructed under the D14DN01B nomenclature. Serial Number 29 was a spare unit which was retained by Oklahoma State University as a possible substitute in the event that one of the systems failed and there was not sufficient time for repairs. A schematic of the Model D14DN01B detector system, OSU drawing D14DN01B, is shown in Figure 11. A chronological tabulation of the systems produced under this contract along with their sensitivity in mgm cm/sec is presented in Table 1 (Page 32). The "A" and "B" scale data are listed separately along with the date and method of calibration. With two exceptions, the "A" scale sensitivity for the D14DN01 systems, when compared to that of the D12DN01B series showed an improvement of at least twenty-five per cent.

5.5 After the production requirements had been fulfilled and several of the detector systems had been used on satellite vehicles, it was decided that the data storage feature which was included in all twenty-eight units was not necessary. This possibility had been considered during the design of the D14DN01 system, and the master printed circuit board had been constructed so the output could be either an "all-event" presentation or the "A" events could be read out in a series of two events per step. The optional selection could be accomplished by altering an electrical jumper arrangement on the master board itself. The decision to convert the units to an all event presentation was based on two significant points; first, the quantity of meteoric materials detected on previous satellites indicated that the influx encountered was not as dense as had been anticipated. Second, the storage feature caused some confusion and erroneous interpretation of the records. All detector systems which had not been used were returned to OSU for "all-event" readout modification.

Some of the systems had been damaged physically due to improper installation and a few had experienced electrical problems. All of these detector systems were to be checked for proper operation, repaired if necessary, modified for an "all-event" presentation and recalibrated

24
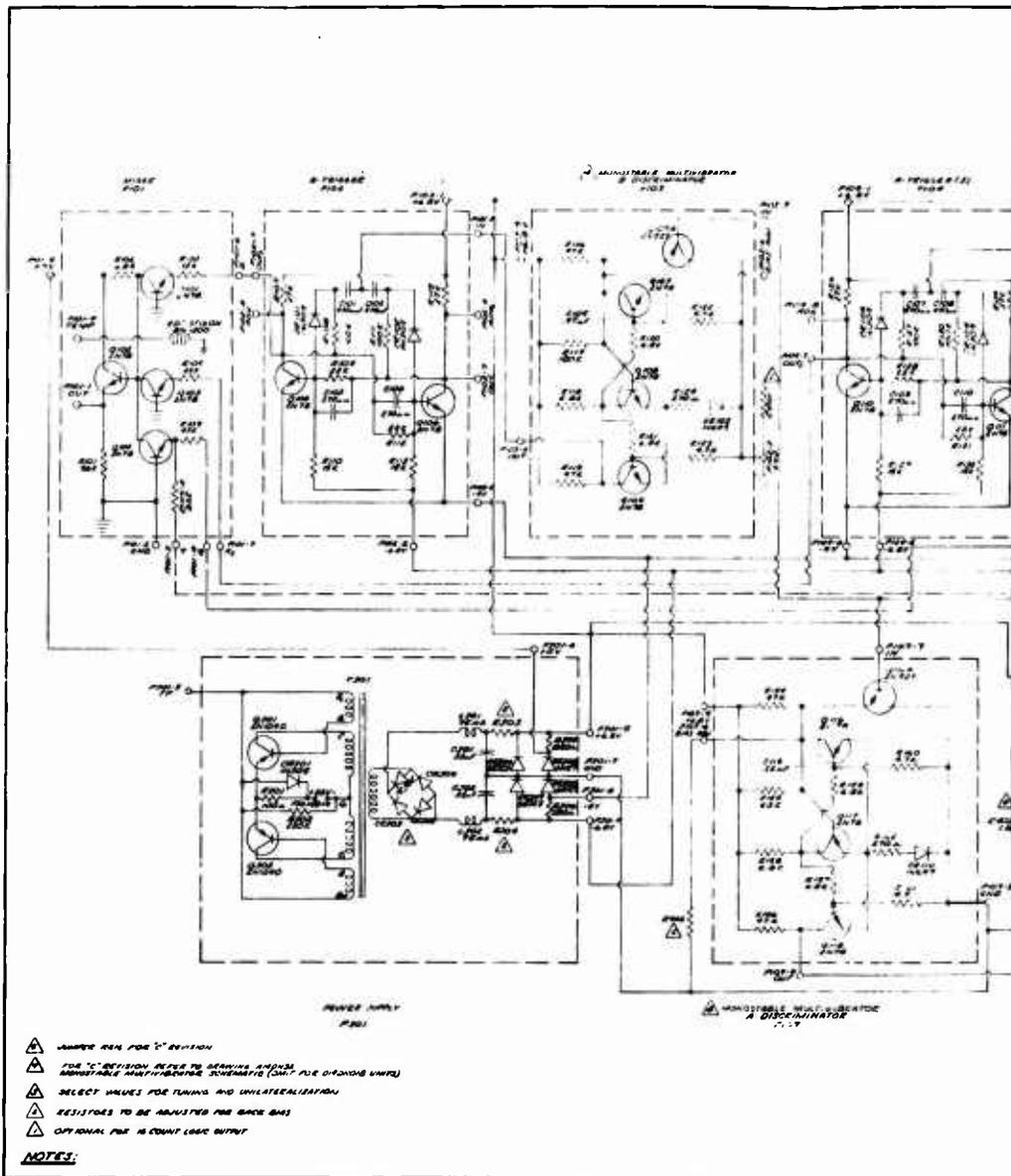
Figure 11. Schematic, D14DN01B Detector System Electronics Package

Schematic, Detector System Electronics Package

D14DN010

2

cs Package
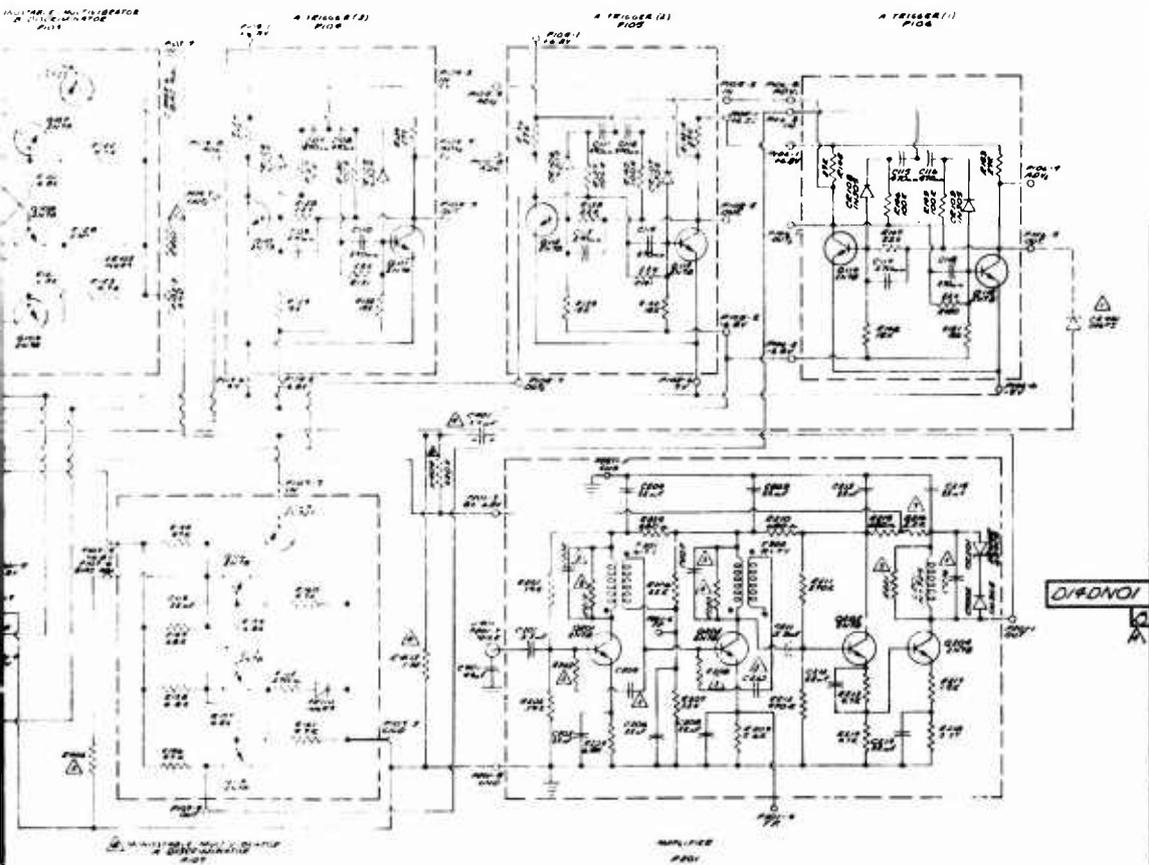
prior to returning them to AFCRL. A total of eleven detection systems were received and surveyed for possible undesirable operating characteristics. Included in this shipment were Serial Numbers 2, 9, and 12 of Model D12DN01B, Serial Number 13 of Model D14DN01, Serial Numbers 17 and 19 of Model D14DN01A, and Serial Numbers 23, 25, 26, 27, and 28 of Model D14DN01F

The initial checkout revealed several problems in the systems, a few of which were inherent in more than one system. The most common indication of failure was detected as a complete loss of "A" or "B" information. As a rule, the amplifier sensitivity was very close to the sensitivity recorded during the original calibration, but the system sensitivity would be very low or one of the information levels would be non-existent. Preliminary investigations served to isolate the difficulty in the discriminator-monostable multivibrator circuit. A comprehensive analysis of the discriminator-multivibrator module provided a sufficient amount of information about the characteristics of the defective subassembly that a logical corrective procedure could be established. The two problems encountered will be analyzed in greater detail.

5.5.1 The semiconductors used throughout the detector system were germanium for the most part. These transistors had been chosen for their higher base to emitter breakdown voltage, typical beta, power requirements and for economic reasons. The germanium transistors are subject to erratic performance when the environmental temperature reaches the hot and cold extremes. However, the temperature ranges set up (-30° C to +60° C) for the detector system had not approached the critical theoretical limits. The phenomenon which caused the detector system to vary in sensitivity was determined to be a combination of excessive collector to emitter and collector to base leakage current in the "off" transistor, Q116, of the discriminator-multivibrator circuit in Figure 13. The resistor, R154, served a dual purpose, since it was the emitter and collector load for Q116A and Q116 respectively. The emitter voltage of Q116A, which could be adjusted by changing the value of R402, determined the threshold sensitivity level for the system. This method of rejection was common to both "A" and "B" discriminators.

When the emitter voltage of Q116A was monitored, a significant variation from the anticipated level was noted. A voltage reduction at this point would tend to lower the system sensitivity level and very low voltage levels would effectively "bias off" the information. The load resistor R154 was 47 kilohms, and a relatively small current drain through this resistor would produce an appreciable voltage drop across it. The combined leakage current of Q116A and Q116 would not affect the system sensitivity under normal conditions, but if either or both of these units develop excessive leakage characteristics, the system sensitivity would suffer. For example, if the total leakage current through this resistor reached 80 microamperes, the emitter potential on Q116A would be lowered from its predicted value of approximately six volts down to two volts. Consequently, the system sensitivity was reduced as a direct function of the leakage current and finally, with sufficient leakage current, the data level would remain fixed at its last binary indication.

27
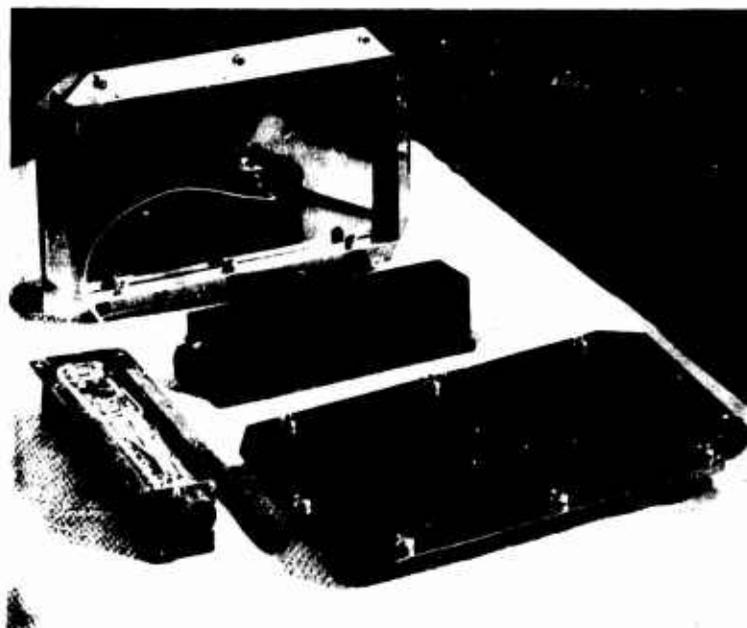
Figure 12. Acoustic Detection System D14DN01A

Figure 13. A-B Discriminator-Monostable Multivibrator
D14DN01B System

5.5.2 The inverter transistor, Q118, also became defective
(i.e., the leakage currents exceeded specifications) on some of the
systems. The general effect of this failure was very similar to a
failure in the discriminator section, but the difference was obvious
when an investigation was made with an oscilloscope. The output level
from the discriminator-multivibrator module became too small to trigger
the bistable multivibrators in the logic section.

5.6 The detector system's operation had not been characterized by
this varying sensitivity level during preliminary checkouts and en-
vironmental testing. The circuits had been designed for "worst case"
conditions and the possibility of semiconductor "aging" offers the only
explanation for the problems encountered. Concrete evidence which
would substantiate this theory would be difficult to obtain, as well as
prohibitive from the standpoint of costs involved. One possible solution
to the problem would be to install silicon transistors, which are more
stable under extreme temperature variations.

The conversion from germanium to silicon transistors could
not be made directly, due to the difference in bias requirements, gain
characteristics, and physical incompatibilities. Additional improvements
could be accomplished by a complete revision of the discriminator section,
concurrent with the transistor conversion for Q116A, Q116, and Q118, by
modifying the existing amplifier-to-discriminator coupling arrangement

29

and adding dc isolation between the discriminator and the multivibrator pulse shaping circuit. The modifications were considered essential to the future reliability of the system, and they were incorporated under the Part No. D14DN01C nomenclature. A brief explanation of the theoretical significance of these changes is given in the following subsections.

5.6.1 By installing a constant-voltage bias arrangement on the discriminator transistor, Q116A, and adding a coupling capacitor on either side of this section, the dc voltage fluctuation due to excessive leakage current in either adjacent transistor was isolated from the discriminator circuit. This preventive measure, coupled with the germanium to silicon transistor substitution, reduced the probability of bias level shifts from the predetermined threshold requirements for optimum sensitivity.

5.6.2 A secondary preventive measure was accomplished by the addition of the coupling capacitor C119 and the collector resistor R155 for transistor Q116, Figure 14. The detrimental effect had been inter-related with the reduced sensitivity discussed in 5.6.1, but it had presented itself as an independent source of marginal operation in the mono-stable multivibrator, Figure 13. The variant potential which was responsible for the fluctuating sensitivity was also the collector voltage for the "off" transistor Q116. When the potential decreased to its lower extremes, it was too low to support the internal regeneration
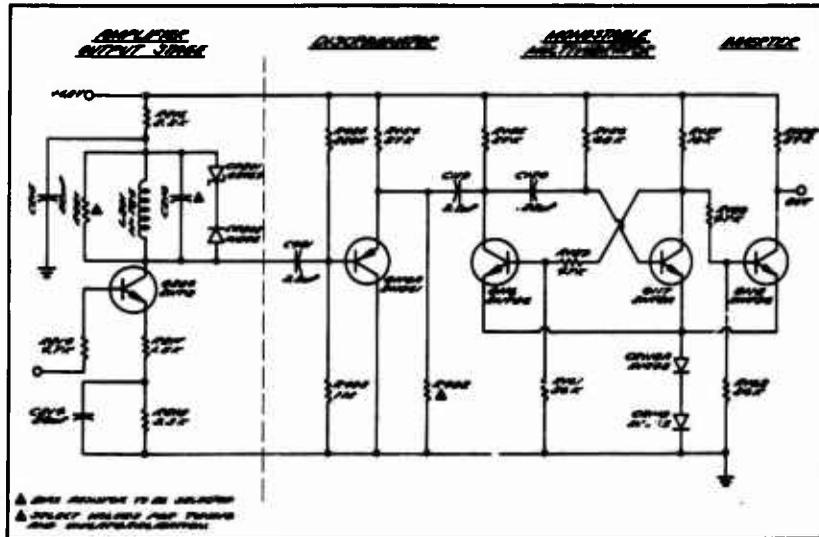
Figure 14. Revised Discriminator - Monostable Multivibrator

necessary for the multivibrator circuit to function properly. The dc
isolation provided by C119 reduced the susceptibilⁱty of failure, due
to low collector potentials, to the leakage current inherent in Q116
itself. The fact that Q116 was changed to a silicon transistor should
enhance the operational characteristics of the multivibrator.

5.6.3 The B+ decoupling network for the amplifier output stage
was modified. Resistor R216 of Figure 14 was shorted out on the back
of the etched circuit card for the amplifier module. The value of R216
had been large in the original design to establish the desired dc bias
level for Q116A. Since the proposed revision was to capacity-couple the
amplifier output into the discriminator, the dc bias was no longer re-
quired. It should be pointed out that a change to a small value for
R216 would have been desirable, but it could not be installed conveniently
without removing the potting compound, with a resulting chance for damage
to amplifiers already completed and fully tested. By shorting the resistor,
the collector of Q204 was allowed a greater voltage swing, which served
to compensate for the increased base to emitter voltage drop of the silicon
transistor which was installed in the discriminator section.

5.6.4 The "A" and "B" monostable multivibrators had been
identical, but due to the bias requirement on the "B" discriminator
portion the emitter resistor for Q116A could not remain the same for
the "A" and "B" units. This was the only difference in the complete
module, and it cancelled the interchangability that had been planned orig-
inally. For the "A" unit, R154 was 27K, and its corresponding value in
the "B" unit was 68K, R116. For optimum operating conditions, to achieve
the desired input impedance for the amplifier output, a value of approx-
imately 27K was required. The bias voltage level for "A" and "B" in-
formation threshold could be adjusted by changing an external resistor,
R402, which set the emitter potential of Q116A. The emitter voltage
required for the "B" discriminator to establish a 1:10 sensitivity ratio,
between the "A" and "B" data levels, was roughly 35 to 40 per cent of
the potential normally at this point for the "A" discriminator. For
most systems, a 39K bias resistor, R402, would accomplish the predetermined
requirements in conjunction with the 68K, R116. The parallel combination
of these two resistors effectively constituted the emitter impedance of
the stage and returned it to the vicinity of 20K to 27K which was desir-
able to establish the proper load impedance for the amplifier.

5.6.5 After several of the revised A-B discriminators had been
checked out successfully, two units indicated a marginal operating
characteristic. The malfunction was detected as a multiple count, which
is definitely an undesirable feature. The symptom was most prominent at
the lower extremes of the temperature range. The output pulse from both
the "A" and "B" monostable multivibrator circuits decreased in time
duration as the temperature was lowered. A finite reduction in the time
constant was expected under these conditions, since the electron mobility
within the semiconductor structure decreases when the unit is subjected
to lower temperatures. This theoretical phenomenon is responsible for
the inherently lower beta factors noted when transistors are operated
below the normal ambient temperature. This explanation exemplifies
precisely the origin of the difficulty which was encountered. Briefly,

31

TABLE 1

LOCKHEED MICROMETEORITE DETECTOR CALIBRATION
SENSITIVITY - MGM CM/SEC

S/N	Model	A SCALE			B SCALE			Date	Bead	Striker No.	CALIBRATION Basis	Ref. Station
		Avg.	Min.	Max.	Avg.	Min.	Max.					
1	D12DN01B	.4	XX	XX	5.00	XX	XX	Oct. 59	Yes	-	25 sta grid	B-3
1	"	.41	.36	.59	3.60	3.4	3.75	28 Apr 60	No	1	"	B-3 & D-3
2	"	.4	XX	XX	5.50	XX	XX	15 Nov 59	Yes	-	"	B-3
2	"	.4	XX	XX	3.75	XX	XX	26 Apr 60	Yes	-	"	B-3
3	"	.32	XX	XX	4.00	XX	XX	Nov 59	Yes	-	"	D-3
3A	"	.30	.2	.4	3.88	2.5	5.33	27 Feb 60	No	D	"	All
4	"	.55	XX	XX	4.00	.XX	.XX	Nov 59	Yes	-	"	D-3
5	"	.28	.16	.37	4.00	XX	XX	Mar 60	Yes	-	"	All & D-3
6	"	.39	.28	.49	2.14	XX	XX	9 Jun 60	No	2	"	All & B-3
7	"	.70	.50	.95	2.17	XX	XX	7 Apr 60	No	2	"	All & D-3
8	"	1.06	.78	1.32	3.09	XX	XX	7 Apr 60	No	2	"	All & D-3
9	"	1.08	.83	1.32	2.28	XX	XX	7 Apr 60	No	2	"	All & D-3
10	"	.33	.26	.46	2.14	XX	XX	9 Jun 60	No	2	"	All & B-3
11	"	.30	.25	.46	2.30	XX	XX	9 Jun 60	No	2	"	All & D-3
11A	"	.30	.22	.37	2.50	2.0	3.0	14 Feb 61	No	D	"	All
12	"	.38	..7	.44	2.00	XX	XX	9 Jun 60	No	2	"	All & B-3
13	D14DN01	.19	.15	.22	1.49	1.04	1.82	11 Nov 60	No	3Y	12 sta grid	All
14	"	.29	.24	.39	3.00	2.48	3.25	27 Oct 60	No	3W	"	All
15	"	.22	.14	.29	1.65	1.05	2.11	12 Nov 60	No	3Y	"	All
16	"	.24	.20	.30	2.00	1.49	2.41	27 Oct 60	No	3W	"	All
17	D14DN01A	.25	.22	.29	2.40	1.83	2.83	28 Dec 60	No	D	"	All
18	"	.22	.18	.30	2.19	1.75	2.66	3 Jan 61	No	D	"	All
19	"	.22	.18	.27	2.10	1.07	2.50	14 Feb 61	No	D	"	All
20	"	.234	.17	.28	2.14	1.75	2.67	14 Feb 61	No	D	"	All
21	D14DN01B	.202	.15	.28	2.02	1.50	2.83	28 Feb 61	No	D	"	All
22	"	.22	.18	.27	1.84	1.42	2.17	4 Apr 61	No	D	"	All
23	"	.167	.14	.18	1.39	1.17	1.67	1 Mar 61	No	D	"	All
24	"	.175	.14	.20	1.9	1.5	2.17	14 Mar 61	No	D	"	All
25	"	.19	.15	.22	1.99	1.5	2.33	14 Apr 61	No	U	"	All
26	"	.23	.17	.28	2.66	1.83	3.33	17 Apr 61	No	U	"	All
27	"	.212	.15	.25	2.69	2.0	2.81	5 May 61	No	U	"	All
28	"	.251	.17	.28	2.68	1.67	2.83	24 Apr 61	No	U	"	All
29	"	.238	.15	.33	2.56	1.67	3.67	7 Jun 61	No	U	"	All

SECTION 1

S/N	Model	A SCALE			B SCALE			Date	Bead	Striker No.	CALIBRATION Basis	Ref. Station
2	D12DN01B	.587	XXX	XXX	3.72	XX	XX	5 Dec 62	No	T	Plate S/N 12	B-1
9	D12DN01B	.455	XXX	XXX	2.25	XX	XX	19 Nov 62	No	T	Plate S/N 12	C-2
12	D12DN01B	.470	.385	.597	2.50	2.11	2.94	20 Nov 62	No	T	12 sta grid	All
17	D14DN01C	.175	.137	.218	1.72	1.27	2.12	15 Oct 62	No	T	12 sta grid	All
19	D14DN01A	.176	.151	.224	1.91	1.20	2.47	21 Feb 62	No	T	12 sta grid	All
23	D14DN01C	.118	.101	.132	1.08	.83	1.27	25 Oct 62	No	T	12 sta grid	All
25	D14DN01C	.124	.095	.152	1.28	.99	1.61	25 Oct 62	No	T	12 sta grid	All
26	D14DN01B	.233	.175	.32	2.6:	1.83	3.35	23 Feb 62	No	T	12 sta grid	All
27	D14DN01C	.155	.118	.184	1.5:	1.19	1.82	5 Nov 62	No	T	12 sta grid	All
28	D14DN01C	.131	.093	.194	1.30	.92	2.12	24 Oct 62	No	T	12 sta grid	All

SECTION 2

the monostable multivibrator is a common emitter type which is biased above ground by the potential developed across two silicon diodes in series in the emitter circuit. The base potential on the "off" transistor cannot rise above the bias level established by the diodes and its own base-emitter voltage drop, except under transient conditions. Under conditions set forth, when the "off" transistor is turned on, it must have enough current gain to produce a voltage drop across its collector resistor which will reduce the collector potential to approximately 1.25 volts.

$$[1.25 \text{ volts} = .6 \text{ volts/diode} \times 2 \text{ diodes} + V_{ce} \text{ (Sat)}]$$

This consistent voltage drop is essential to produce an approximately equal time constant over the temperature range. The "off" transistor must saturate each time it is triggered and the collector resistor must be large enough to drop the voltage to the desired level, even though the reduced beta has lowered the magnitude of the saturation current. In the event that the "off" transistor draws current momentarily during the normal response period but fails to saturate, the time constant is dependent solely on the length of time that this transistor draws current.

The typical amplifier response from a simulated micro-meteorite impact has a symmetrical envelope of 100 kilocycle oscillation. (A replica of this phenomenon is presented in Appendix I, Figure 4-4.) The practical bias level for noise rejection on the "A" level was fixed at approximately 0.5 volts. The monostable multivibrator's time constant was set for approximately six milliseconds, so that the decaying portion of the amplifier response would not trigger the multivibrator more than one time per impact. Spurious multiple counting was a result of the reduced multivibrator time constant actually permitting it to be "cocked" and triggered a second time during the duration of a single impact response from the amplifier. The collector resistor and the base voltage divider resistors for Q116 were adjusted to assure proper operation under "worst" case conditions.

5.7 The modifications which have been described in the preceding subsections were incorporated on five Model D14DN01 micrometeorite detector systems and their nomenclature was changed to Part No. D14DN01C for identification purposes. The five revised systems include Serial Numbers 17, 23, 25, 27, and 28. All the revised systems showed a definite improvement in system sensitivity; some were improved by as much as 40 per cent. The final calibration sensitivity is tabulated in Section 2 of Table 1.

An unwieldy task was encountered when the "C" revision was made a permanent alteration to the existing D14DN01B official drawings. Since several D14DN01B systems were in use by now, it was decided that the logical method for handling the modification would be to use the "overlay" concept on the D14DN01B detector system schematic, OSU drawing D14DN01B, Figure 11, to produce controlled prints of the revised D14DN01C system. Oklahoma State University drawing A14DN32, Figure 15, shows the schematic of the monostable multivibrator-discriminator overlay.

33

This circuit was cut out and affixed to the OSU drawing D14DN01B, over-laying the earlier multivibrator-discriminator circuits, to construct a schematic of the electronic circuits included in the D14DN01C micro-meteorite detection system. The results of the overlay technique are shown in Figure 16, which is the micrometeorite detection system, Model D14DN01C, electronics schematic diagram.

Figure 15. Discriminator-Monostable Multivibrator Overlay for D14DN01C Revision

6.0 MICROMETEORITE DETECTOR SYSTEM CALIBRATION

6.1 The method of momentum calibration, which was used on the early model of the D12DN01B micrometeorite detection systems, had been developed prior to the existence of this contract. This development work was performed under Contract AF 19(604)-1908, and a detailed analysis of the technique is given in the Final Report. (Ref. 1) Briefly, the cali-bration was performed by dropping small spheres of glass of accurately known size onto the detecting plate from some calibrated distance. Since

Figure 16. Schematic, D14DN01C Detector System Electronics Package

35

SCHEMATIC, DETECTOR
SYSTEM ELECTRONICS Pkg.

DI4ONOI

es Package

this technique was very sensitive to the condition of each bead and to the manner in which the bead struck the plate, the operation was tedious and up to one hundred bead-drops were often required to establish the sensitivity of one typical point.

6.2 A new method of calibration was developed under Contract AF 19(604)-7202 and was described in the Final Report for that contract. (Ref. ?) The new technique employed a device which was given the descriptive name "Electronic Striker." The electronic striker was designed to produce a repeatable test whereby a point source of mechanical impact could be produced at a specified point upon the surface of a sensor assembly. The electronic striker utilizes a pulse generator capable of producing pulses of the desired shape, with a variable amplitude. These electrical pulses are then applied to a bimorph-type piezoelectric transducer element, which responds with a flexure in the bimorph element. A sapphire or diamond conical tip mounted at the free end of the bimorph element could be used to produce mechanical stimuli on the sensitive surface of the detection plate. The amplitude and velocity of the stylus motion is related to the shape and the amplitude of the electrical driving impulse. Stylus motion against the plate then represents a momentum stimulus applied to a known point and mechanical energy propagates through the material to the microphone mounted against the plate.

In the course of development of the calibration technique finally employed, a short investigation was made into the mechanism by which the plate microphone sensor combination responded to these point momentum stimuli. A tentative hypothesis of multipath propagation effects, (wherein the direct signal path from point of impact to the sensitive area of the microphone face was modified by energy reflected from points of discontinuity at the boundary of the plate or support points on the plate) was established and interference effects were verified under laboratory conditions with a test plate of large area. Details of this investigation have been reported elsewhere under an associated contract. (Ref. 2) Although it was originally assumed that this energy was propagated as a Rayleigh wave, direct measurements of the velocity of propagation disclosed this was not the predominant mode and that fundamental propagation through the plate was in the simple shear mode. Attempts to eliminate reflected energy and associated interference effects as a source of ambiguity in the exact value of momentum stimulus to be attributed to a given electrical output met with failure. However, it was discovered, in the course of the investigation, that the interference effects from boundary reflections actually assisted in achieving statistically more uniform sensitivity over the major area of the plate.

6.3 The bead-dropping technique was used to set up a reference for the electronic striker calibration. A standard amplifier and microphone combination were set aside for the calibration process. The bimorph crystal element was susceptible to variations after a few weeks of operation, and it was necessary to check the striker calibration prior to each sensitivity check of the micrometeorite detection systems. This method of calibration proved very practical for obtaining accurate sensitivity data, with a reduction in the overall effort required.

6.4 The sensor plates for the Model D12DN01B units were laid off in a five-by-five coordinate arrangement. The basic plan was to establish a sensitivity level for all 25 grid points and average these for the mean system sensitivity. It was a recognized fact that each point on the plate would possess an individual sensitivity level due to the non-homogenous characteristics in the plate itself and the magnitude of the reflected impact stimulus from the various edges of the detecting surface. The bead dropping method proved to be impractical for the 25 point calibration. After the development of the electronic striker, the 25 point calibration became a reality. As a result of subsequent investigations, the 25 point grid system was reduced to a 12 point arrangement.

6.5 The experience gained through the development and use of the electronic striker led to the exploration of the acoustic detector sensor system sensitivity as a function of the point of impact.

6.5.1 The assumption had been made earlier that the momentum of a given particle was linearly related to the output of an ultrasonic microphone in contact with the surface against which the incoming particle impacted. As a measure of the detectable threshold momentum, certain calibration factors were assigned to each system. In general, the sensitivity has been rather crudely defined in terms of some "average" value of momentum which could reasonably be expected to provide enough electrical energy to overcome the detection threshold of the associated electronic package. It had not been found possible in earlier investigations to isolate the experimental error of the calibration technique from the variation in sensitivity as a function of the impact point upon the surface of the collecting plate. The advent of the electronic striker made available a tool for a more thorough exploration of the variation in sensitivity as a function of the point of impact.

6.5.2 The general objectives of this particular investigation can be broken into two separate categories. First, a more adequate determination could be made concerning the variation in sensitivity over the entire surface of the detecting plate. Better knowledge of the relationship between the point of the impact and the true sensitivity might possibly provide a clue towards a design refinement for the collecting system. Second, a more adequate determination of the mean sensitivity of a typical plate was desired as a check against the validity of the earlier procedures employed for calibration. The standard method of calibration on recent versions consisted of a determination of the sensitivity at 12 selected reference stations. The mean sensitivity was then defined as equal to the average of these 12 selected points. The 12 reference points were not randomly selected, but were based on earlier knowledge of the general form of the sensitivity distribution function. (Crude studies with bead-dropping disclosed that a highly sensitive region existed in the immediate vicinity of the microphone, and that the average sensitivity remained reasonably constant over portions of the plate more than two inches removed from the point at which the microphone attached.)

6.5.3 The sensor assembly selected for this investigation represented a typical unit as defined by OSU drawing No. C12DM01A, Figure 1.

38

Microphone No. 13-2 was selected as typical of those microphones available for use with systems currently being fabricated. In addition, the microphone was installed against the undersurface of the collecting plate by the standard method. A force of three pounds was used during the cure period for the cement in order to achieve the optimum sensitivity for the microphone in question.

The technique of exciting the microphone was selected only after some study and consideration of those types of data most feasible for the large number of points to be involved. A test of the plate in question and the associated test amplifier indicated that the output from the system remained a linear function of the mechanical stimulus applied over a region extending from -0.05 volts to -1.15 volts peak at the test amplifier output terminal. With this wide linear region available, it was decided to use an arbitrary and constant mechanical stimulus which provided an output level near the center of this linear region. The amplifier output voltage amplitude was recorded as a function of impact position on the surface of the plate, rather than the stimulus necessary to provide a constant reference output voltage level from the system. This choice of the method of investigation was justified by the prior establishment of a linear relationship between output voltage and applied stimulus.

The preliminary investigation established that, over a 23:1 range in output level, the negative peak excursion was linearly related to the input stimulus.

$$-\hat{e}_{out} = (-K) \quad p_{stimulus}$$

If the stimulus was then held constant (p_{test}) in level and the position at which the stimulus was applied varied over the surface of the plate, the system sensitivity variations were detectable as variations in the output level.

$$\frac{-\hat{e}_{threshold}}{-\hat{e}_{out}} = \frac{-K}{-K} \quad \frac{p_{threshold}}{p_{test}}$$

$$p_{threshold} = p_{test} \left(\frac{\hat{e}_{threshold}}{\hat{e}_{out}} \right) = \left(p_{ref} \, \hat{e}_{threshold} \right) \left(\frac{1}{\hat{e}_{out}} \right)$$

By prior establishment of values of p_{ref} and $\hat{e}_{threshold}$, it was a simple matter to convert the raw data (in the form of negative amplifier output voltage at a given point of stimulation) to the momentum threshold at that point, since a simple inverse relationship held over the region to which the test was confined. The points used in the analysis gave output voltages ranging from -0.08 to -1.2 volts peak. Excluding a single point over the microphone and a single low sensitivity point near one corner on the plate, the range of output voltages was only -0.10 to -0.90 volts, justifying this simple approach to the analysis. This permitted a considerable simplification in the test set-up in

39

that a constant stimulus could be provided to the electronic striker, and the peak negative excursion of the signal impulse at the amplifier output terminal could then be recorded as inversely proportional to the overall system momentum sensitivity threshold. In order to facilitate the recording of data, the information was presented as a vertical deflection on the face of a cathode ray tube. The horizontal positioning on the face of the cathode ray tube was adjusted to correspond to the lateral displacement of the impact point along a line parallel to the major axis of the collecting plate.

A grid system was provided, based upon increments of 0.25 inches along an orthogonal system parallel to the two axes of symmetry for the collecting plate. A holding jig was devised with parallel reference straight edges graduated in one-quarter inch divisions, along which the striker carriage could be moved in even increments. Transfer of the striker carriage from one such parallel guide to the next then provided a second series of points, separated 0.25 inches with respect to their neighbors. Because the reference grid system had as an origin two edges of the plate, it was discovered that no points hit directly over the microphone. As a result, two extra series of points were taken along mutually perpendicular lines which intersected at the center of the microphone. The grid system used provided a total of 1,390 possible points on the surface of the rectangle whose major dimensions were identical to that of the sensor plate. Of these total possible locations, 26 were excluded by removal of the corners (Ref. OSU drawing C12DM03) which had been cut from the sensor plate to break up reflected energy and permit more uniform sensitivity characteristics. Of the remaining 1,364 points, a total of 61 were inaccessible with the striker mechanism in use because of mechanical interference with the grommet support structures located at eight points around the edge. A total of 1,303 points within the reference grid system were thus accessible for evaluation.

A Polaroid Land camera was used in conjunction with a Tektronix Type 535 Oscilloscope to record the sensitivity as a function of displacement along each of the reference grid lines. Since the vertical deflection was proportional to the voltage output and the horizontal deflection proportional to displacement along each reference grid line, a bar graph proportional to system sensitivity along each grid line was obtained in the photographic recording process. The voltage amplitudes were then read out from the permanently recorded calibration data and tabulated for use in analyzing the sensitivity of the system. It should be noted that the bar graphs represented the reciprocal of the momentum sensitivity, since peak output voltage was recorded for a constant stimulus. Since this was the simplest way of taking the large quantity of prime data needed within a short interval of time, it was decided to process the raw voltage data statistically then convert to the reciprocal momentum values after analysis of the results obtained.

6.5.4 The data in the form of the number of readings obtained for a given voltage output are presented in Figure 17 as a bar diagram showing a frequency of occurrence versus the magnitude of the output voltage. As is evident from inspection of Figure 17, a considerably

40
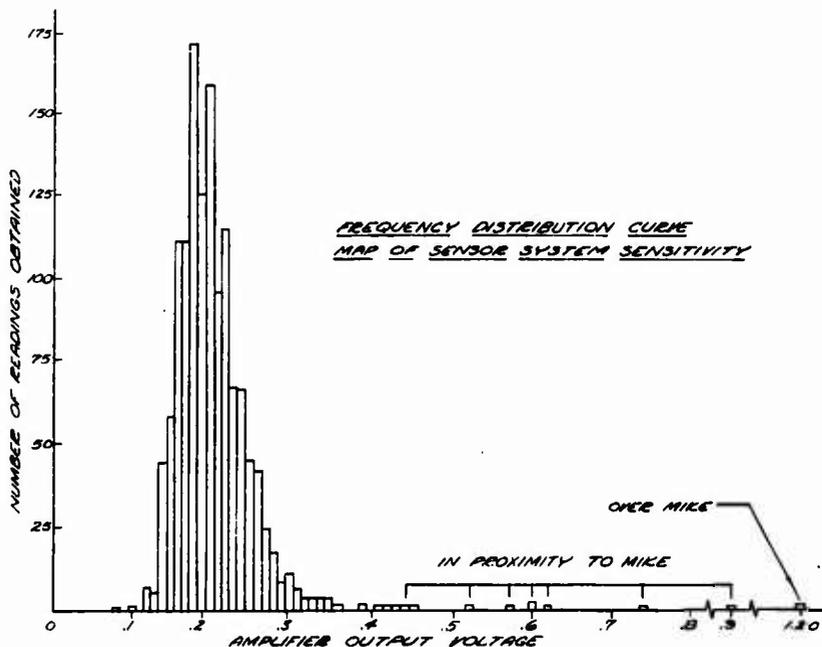
Figure 17. Frequency Distribution Curve Map of Sensor System Sensitivity

greater number of even values of voltage were recorded than of odd values. The reference overlay grid used on the cathode ray tube was divided into increments of .02 volts per division, and it was apparent that an inherent tendency to read to the nearest reference grid line had colored interpretation of the photographic data. The raw data relating frequency of occurrence to voltage output was consequently smoothed before applying analytical techniques. Smoothing was accomplished by the standard technique, in which the frequency of a given interval was doubled and summed with its two adjacent neighbors. One-fourth of this sum was then used as the most likely true value, and an adjusted frequency diagram was plotted and is presented as Figure 18. On the same curve, for reference, are plotted the distribution for odd voltage readings and for even voltage readings. It should be noted that a number of points of relatively high voltage output occurred and are

41
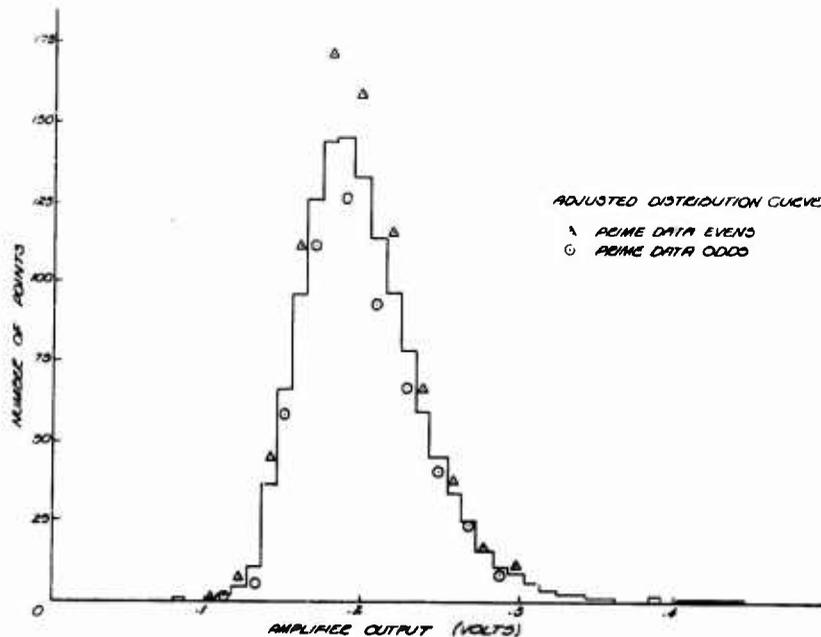
Figure 18. Adjusted Distribution Curve Sensor System Sensitivity

shown at the extreme right-hand edge of the frequency diagram. These points represent those points immediately over and in close proximity to the microphone location.

Statistical analysis of the data was carried out on two bases. First, considering all reference grid points, the mean value was calculated as -0.204 volts. The standard deviation was found to be 0.0605. From this analysis, 91.46 per cent of all readings were predicted to lie between -0.100 and -0.308 volts peak. This prediction was based upon an assumed Gaussian distribution of the data; study of Figure 18 indicates that the data actually were skewed in such a direction as to compress the deviation at the low output voltage end. For comparison purposes, a second analysis was run excluding those nine points in immediate proximity to the microphone location. This procedure was justified by the fact that a relatively simple physical system could be devised to desensitize a plate over this area if a sufficient improvement in uniformity of response could so be achieved. The analysis under these

42
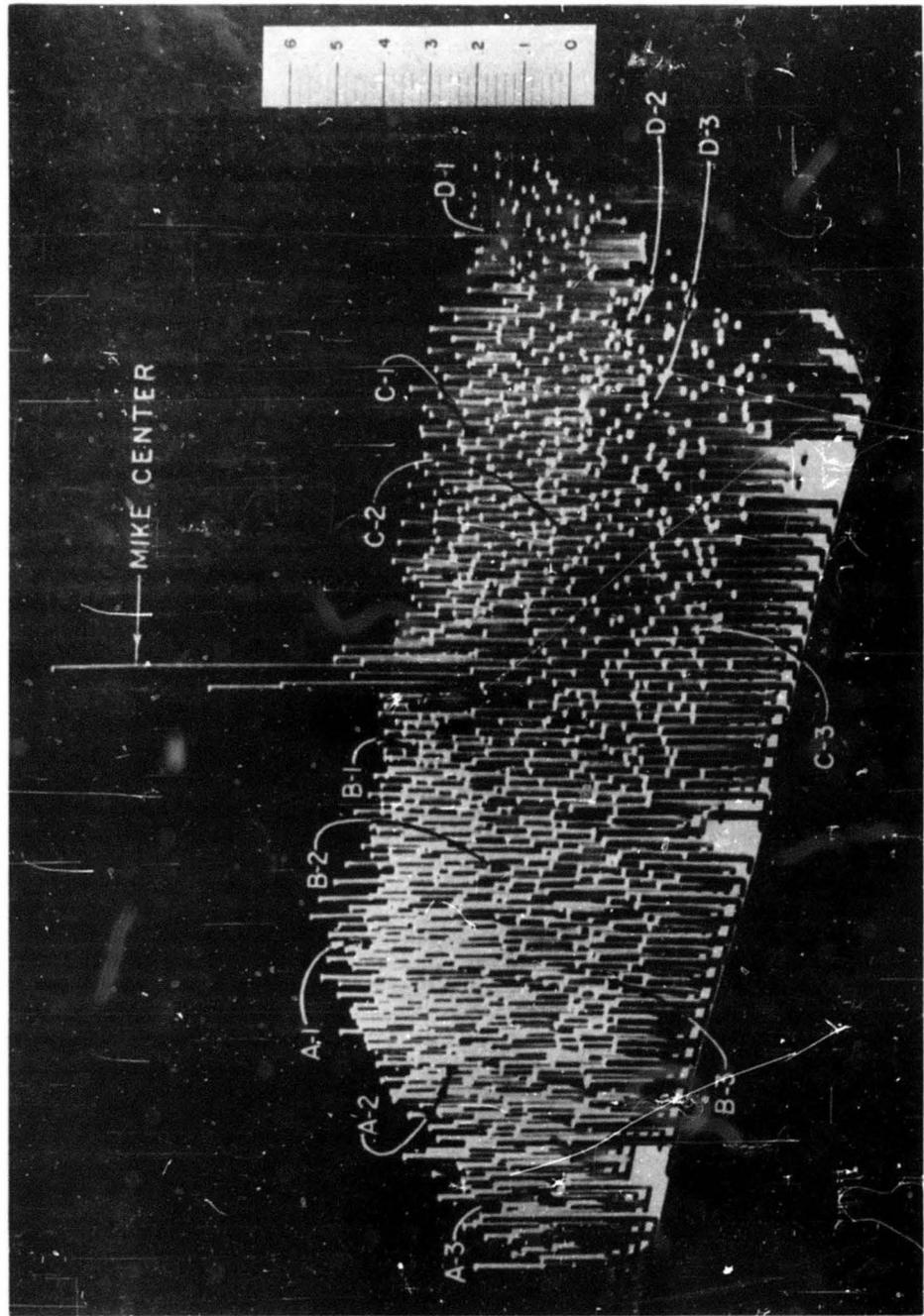
Figure 19. Scaled Model of Sensitivity Versus Impact Position

43

circumstances then reduced the total number of points to 1,294 for which the mean value was -0.201 volts. The standard dev'ation was reduced to 0.0414 by excluding these extremely high sensitivity points and thus 91.46 per cent of all readings were predicted to lie between values of -0.130 and -0.272 volts peak.

For comparison purposes, those 12 points which correspond to the 12 reference stations in prior use as calibration stations were averaged and found to yield an average sensitivity of -0.198 volts; excellent agreement with the statistical analysis may be noted. The range for the 12 points in question was from -0.140 volts to -0.350 volts; of these 12 selected points, that of -0.35 volts (which was obtained at station D3) was regarded as somewhat questionable, but represents a typical determination by the older method.

As an aid to visualization of the overall sensitivity contours, a three dimensional model of the results of this investigation has been prepared and an oblique view is included as Figure 19. In this model, the height of each peg corresponds to the voltage of the output terminal of the amplifier, while its location on the surface of the plate corresponds to the point under investigation. For reference purposes, the location of the microphone, the microphone attaching screws, and the eight supporting grommets are shown. Aside from the clearly pronounced peak immediately over the microphone, no definitely discernible pattern to the location of points of maxima and minima of sensitivity is evident from casual inspection of the model. The 12 reference stations are also indicated in Figure 19.

Because data has been considered in the form of voltage output for a given stimulus and the true desired end point of this investigation was an evaluation of the momentum sensitivity of the system under test, data have been converted from voltages to momenta. Figure 20 represents a plot of the inverse of the frequency diagrams previously shown in which the number of readings corresponded to a given momentum threshold have been plotted versus the momentum threshold. The smoothed curve is presented with points defining the odd and even data discussed previously for reference purposes.

6.5.5 As an aid to interpretation to the validity of the calibration technique employed, the Table 2 of this report lists the maximum and minimum momentum threshold obtained for several cases. Figures are quoted for the distribution of all points, including those nine immediately over the microphone, and also for the alternate analysis which excludes the nine highly sensitive points. As a measure of the confidence with which the calibration can be accepted as representative of the total area of the plate, points have been successively excluded from both the maximum and minimum sensitivity ends as designated in the table. The first entry is for all points under consideration; each successive entry has then had points excluded to represent the percentage of the total points lying between certain extremes of momentum sensitivity. For comparative purposes, the final entry of the table presents similar analyses of 12 discrete points formerly used. Values are tabulated for the average value and the maxima and minima, both for all points and for the alternate analysis excluding the bad point at Station D3.

44
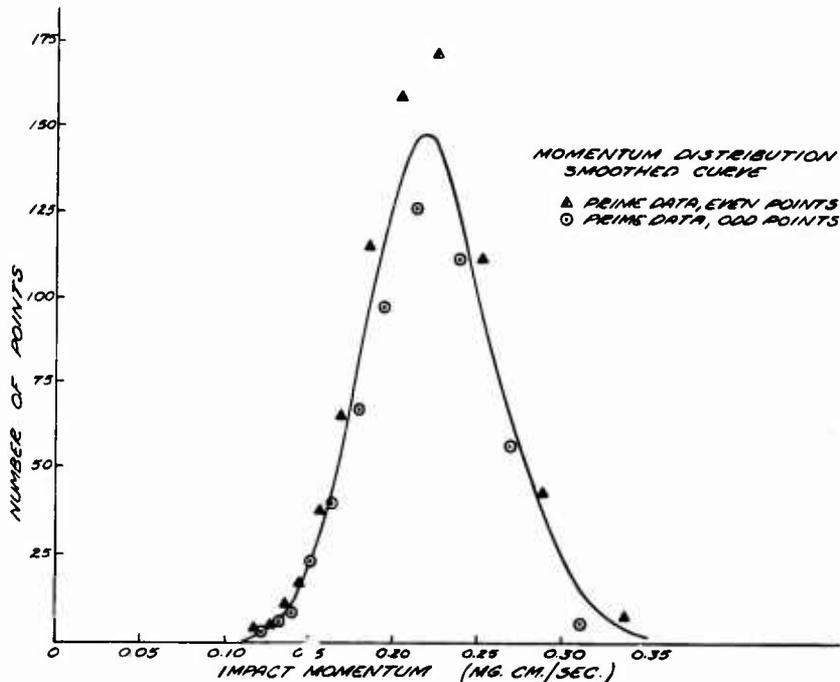
Figure 20. Momentum Distribution Smoothed Curve

It should be emphasized that the variations in sensitivity reflected in the following table do not represent errors in the measurement technique, but rather real differences in sensitivity distributed about the surface of the plate. The postulated mechanism indicates that a random phase relationship which exists between the main incident acoustical energy, as compared to that following various reflected paths (as shown in Figure 21) may result in cancellation or addition effects at the microphone location. Experimental verification of the qualitative theory is available in the form of photographs of the electrical output for a given mechanical stimulus as the point of the stimulus is varied about the plate. Locations near the microphone, where the direct wave has a much smaller path difference than any possible reflected wave, indicate that the maximum energy occurs almost immediately after application of the mechanical stimulus. In contrast, the amplifier output

45

TABLE 2

Tabulated Range of Detectable Momenta over Surface of

C12DM01B Sensor Assembly ($\frac{mgm\ cm}{sec}$ units)

(Tabulated figures are minimum and maximum values observed in original experiment; smoothed distribution function correction is not applied except in case of statistical prediction of range for 91.47 per cent of readings.)

Percentage of Total Points which Fall within Range	1303 Points P mean = 0.196 $\frac{mgm\ cm}{sec}$ Std. Dev. = 0.605	1294 Points (Excluding 9 over Microphone) P mean = 0.199 $\frac{mgm\ cm}{sec}$ Std. Dev. = 0.414

	P min	P max	P min	P max
100%	0.033	0.500	0.091	0.500
99%	0.077	0.333	0.108	0.333
98%	0.102	0.308	0.114	0.308
97%	0.114	0.286	0.125	0.286
95%	0.129	0.286	0.129	0.286
90%	0.138	0.266	0.143	0.266
91.47% Tab	0.138	0.266	0.143	0.266
91.47% *	0.130	0.400	0.147	0.308

12 Standard Calibration Stations

All 12 points	Excluding Station D-3
P mean = 0.206	P mean = 0.219

P min = 0.117	P max = 0.291	P min = 0.186	P max = 0.291

* Statistical prediction is based upon assumption of Gaussian distribution for smoothed data. Skewed nature of data is evident in deviation between actual P max and predicted P max.
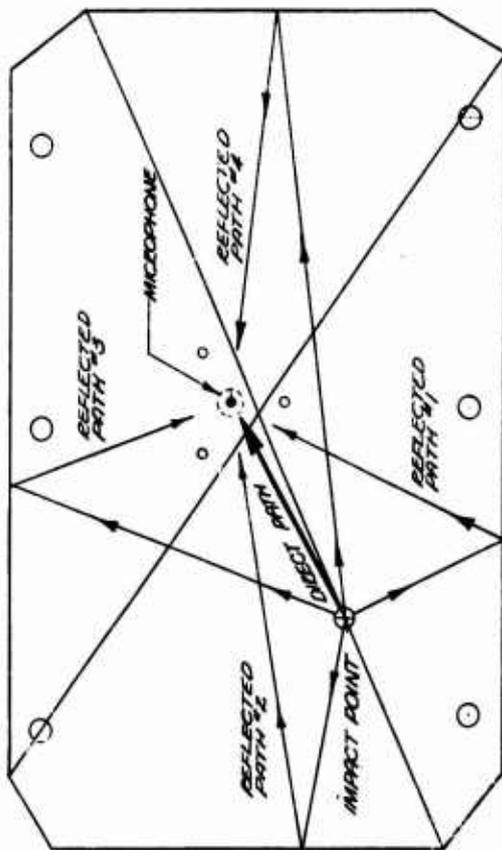
Figure 21. Diagram of Multipath Propagation Effect

47

waveform for striker locations near the edge of the plate frequently
indicate that the maximum electrical response occurs at a time appreciably
later than the application of the impulse, where multi-path propagation
effects eventually result in a phase additive condition at the micro-
phone location.

An interpretation of this phenomena, taken in con-
junction with the diagram of sensitivity versus frequency of readings
obtained in this investigation, would indicate that the true mean momentum
sensitivity for the system in investigation was in the vicinity of 0.215
mgm cm/sec and that this figure would be disturbed by reflected energy
to the extent that fluctuations within the region of 0.12 to 0.33 mgm cm/sec
might reasonably be expected if a reflected signal of approximately one-
half amplitude resulted in either reinforcement or cancellation effects
at the microphone location.

6.5.6 As a result of this investigation, it has been con-
cluded that a simple system of averaging 12 discrete readings dis-
tributed properly over the surface of the plate suffices to define the
mean system sensitivity for units of this particular mechanical design.
Excluding the small area immediately over the microphone, the momentum
threshold for the major surface of the plate may be expected to vary by
approximately $\pm$ 55 per cent of the mean value over 99 per cent of the
total area of the plate. A variation of $\pm$ 30 per cent exists for about
90 per cent of the surface of the plate. The exclusion of the extremely
sensitive region directly over the microphone will involve a loss of only
about one-half of one per cent of the total effective area of the sensing
system. if the area over the microphone is not excluded, the variation
anticipated over 99 per cent of the plate area increases to approximately
$\pm$ 65 per cent, but remains $\pm$ 30 per cent for 90 per cent of the surface.

Based upon the results of this investigation the standard
method of calibration was simplified to a 12 point grid system, beginning
with Serial Number 13. Calibration results were presented in Table 1.

7.0 ANALYSIS OF DATA RECEIVED UNDER FLIGHT CONDITIONS

7.1 Although this particular contract was not intended to embrace
reduction of the data on micrometeorite influx obtained through use of
the equipment, this organization was naturally interested in the per-
formance of the equipment under flight conditions. Unfortunately, little
data received from the systems were available to OSU for analysis.
Arrangements were made to obtain copies of the information recorded at
ground receiving stations from the flight of one satellite vehicle
which incorporated three of the systems described in this report. All
three of the systems were Model D12DN01B, and were flown in a multiple
installation on test Vehicle No. 2909 which was launched on 31 January
1961 from Vandenberg Air Force Base. The vehicle has since been
designated officially as satellite 1961α1. The available analog data
strip chart records from various receiving sites, decommutated and pre-
sented with system time code, were supplied to OSU for study in order
to determine whether or not the systems were functioning as desired.

48

Some preliminary conclusions from this same satellite have been reported earlier by AFCRL. (Ref. 7) In this report, some preliminary results from 1961ω1 were compared with data achieved from similar systems installed on satellite 1960ζ1. The acoustical detection equipment on 1960ζ1 was not identical to that reported in this instance, but comprised two different instrumentation systems for detecting micrometeorite influx. Data from the two satellites were in reasonable agreement and further details may be noted in the reference sited.

The attempt to obtain a more definitive interpretation of influx rates (based upon all available records from satellite 1961ω1) was undertaken as an indirect result of attendance at the International Symposium on the Astronomy and Physics of Meteors, held in the latter part of August 1961 at Cambridge, Massachusetts. During this symposium, a number of strip chart telemetry records with raw influx data covering Orbits 1, 2, 5, 6, 7, 8, 9, 13, 14, 15, 16, 17, 22, and 23 for this particular vehicle were obtained for more detailed study. Several factors of importance in obtaining a definitive analysis of the meaning of the basic telemetered data became evident upon first inspection of these strip charts:

7.1.1 A clearly recognizable periodicity of data pulses existed on one of the three channels of telemetry. The period was approximately 30 seconds; more exact determination was limited by the one second resolution capability of the decommutated telemetry record.

7.1.2 A relatively large number of time-coincident events were noted for certain pairs of the telemetry channels. These time-coincident events appeared to correlate with the characteristic 30-second periodic signal noted on the channel mentioned above.

7.1.3 The availability of real-time coding allowed precise determination of the exact time at which records were received. Overlap occurred between several of the individual strip charts. This permitted extension of the total time of real data available for a given orbit in three instances (Orbits 1, 2, and 16). It also allowed correlation between records for more than one receiving site in order to identify extraneous noise signals which had been generated through failure of synchronization in the decommutation equipment. The fact that these overlap regions frequently included data pulses meant that the earlier analysis, which assumed all strip charts were independent recordings, had been in error by interpreting duplicated signals as separate events.

7.1.4 Later information available (since early studies of 1961ω1 date were undertaken) permitted identification of the specific serial numbers of the three systems involved and correlation with the physical location of each on the payload package. This information also permitted establishment of threshold sensitivity limits for the individual telemetry channels. The locations and telemetry channels specified for the micrometeor systems in this and subsequent sections of this report are specified according to information received from Miss Lois Della Lucca, CRZAD, of AFCRL.

49

7.2 An evaluation of the micrometeorite influx data was undertaken for two reasons:

7.2.1 The primary goal was to provide as valid an interpretation as was reasonably possible for the true influx rates indicated by the three new systems in question, taking into account all known factors involving calibration of the equipment and the elimination of spurious events mixed with the real data.

7.2.2 A secondary purpose was to evaluate system performance as evidenced by these records. As an aid in evaluating these data with reference to earlier studies, the best available information from the earlier rocket experiments performed under AF 19(604)-1908 was rechecked. New influx figures were computed, utilizing the latest corrected readout for the original real time records from the rocket flights in question.

7.3 As an aid to interpretation of the records, the following summary of the nature of the data is pertinent:

7.3.1 The model D12DN01B system uses a metallic sensing surface in contact with an ultrasonic microphone. An electrical output signal from the microphone (which is proportional to the momentum of any particle impinging upon the surface) is fed through an amplifier to two amplitude discriminators, each of which will pass signals of amplitudes greater than that produced by some arbitrary momentum threshold. The signals which exceed the threshold are passed through to a set of binary storage registers. The lower amplitude threshold only is passed when an "A" event is detected, whereas a larger particle momentum value will produce a "B" event signal passing through the second discriminator as well. Three cascaded binary stages give a total storage capacity of eight "A" events before recycling, while a single binary gives a storage capacity of only two "B" events before recycling. The output voltage from the system mixes DC signals from the last two binary stages in the "A" register with the "B" register output in such a manner as to provide one of eight discrete output voltage levels. Because the state of the first binary in the "A" register is not readable with this system, the output voltage level advances only every other time an "A" event is detected, but changes with each detected "B" event. The odd "A" events which do not advance the output voltage level are referred to as "hidden A" events; they are detectable only by inference when the next following signal does advance the output voltage to a new level.

7.3.2 The output signal from each system was transmitted from the vehicle in a time-sequential commutation of the telemetry signal. Data sampling was at a rate of one per second. Received signals, together with a time code, were recorded on magnetic tape at special stations located at Kodiak (Alaska), Vandenberg Air Force Base (California), Hula (Hawaii), and New Boston (New Hampshire). The tapes were then played back, decommutated, and oscillographic strip chart records supplied for analysis. Several decommutated channels were interleaved on each strip chart, including the desired data on channels 38, 40, and 42. Random choices of deflection scale factor and position for these channels, as well as variable paper speed, complicated the analysis of

the data. The recording of system time in a simple binary code, together with pre-playback, three-point calibration and post-playback, five-point calibration of each channel, allowed identification of the horizontal and vertical scale factors applicable to a given channel on a given strip chart. Occasional sequential interruption of the light beams used in the oscillograph proved helpful in trace identification when the interleaved channel records crossed one another, but left some ambiguities in the case of simultaneous level switching on more than one channel. These ambiguities were resolved by considering the possible logical sequences permitted by the instrumentation.

7.3.3 The vehicle was positioned for a stable attitude in orbit, directed with the nose downward (toward the earth) and with a slow spin rate. A relatively circular polar orbit of about 500 kilometers in altitude was achieved.

7.3.4 Two sensor assemblies were installed parallel to the longitudinal axis, diametrically opposite one another near the middle of the payload, with the plane surfaces of the sensor assembly thus approximately perpendicular to the direction of orbital motion. One system, Serial Number 4, was adjusted for momentum threshold levels of 0.55 mgm cm/sec for "A" events and 4.00 mgm cm/sec for "B" events. The output of this system was fed to channel 38 of the telemetry. The second lateral sensor, Serial Number 5, had an "A" threshold of 0.28 mgm cm/sec and a "B" threshold of 4.00 mgm cm/sec; telemetry was via channel 40. A third detection system was mounted with the surface perpendicular to the longitudinal axis of the payload at the aft end, and thus directed outward with respect to the surface of the earth. This system, Serial Number 8, was telemetered on channel 42 and had been adjusted for an "A" threshold of 1.06 mgm cm/sec, with the "B" threshold set at 3.09 mgm cm/sec.

7.4 Recovery of data from the strip chart records was straight forward, although somewhat tedious because of manual reduction techniques.

7.4.1 The first step in analysis of the telemetry data was to identify the exact system time for each available strip chart from each station on the various orbits in question by making use of the "system time" code. Voltage output levels as a function of time for each channel were obtained using the pre-and post-recording calibrations for individual deflection factors. A master strip chart which included all available data, both real and spurious, was prepared, with all three channels separated vertically and drawn to identical scale factors for time and channel voltage excursion. This step permitted quick visual identification, both of periodic signals and of time-coincident signals on more than one telemetry channel. The exact system time of occurrence of each event was noted immediately above the change in telemetry voltage level which indicated the event on the decommutated signals. Overlap periods for simultaneous recordings at more than one station were thus automatically compensated for by plotting to a "system time" scale. The scale factors chosen for presentation were such that approximately 30-second spacing (or multiples thereof) would fall on major time divisions of the master chart, thus facilitating identification of those events

which had appeared periodic in nature upon first inspection. Replotting to a constant voltage scale factor for all records also permitted identification of all eight possible signal output levels for each of the three systems. Knowledge of the logical sequence for these output levels permitted some "gap-filling" during periods of loss of synchronization within individual station records.

7.4.2 The raw data presented on the master chart were examined carefully and all possibly periodic events on channel 42 were identified. It was noted immediately that the periodicity was such that events spaced at 30 seconds (and multiples of 30 seconds) were occasionally evident on the chart record. In every case the so called "hidden A" register value corresponding to an unread (odd numbered) "A" event was found to account for the "skipped" 30-second spurious impulses on the output from channel 42. Beginning with Orbit 2, a spurious event occurred every 30 seconds on channel 42. Identification of all the system times at which one of these interfering sequence of pulses might be expected to occur within each segment of data available then permitted identification of those observed spurious events recorded on channels 38 and 40.

7.4.3 Once this identification had been achieved, it became possible to prepare charts from the composite record indicating the number of "false B" events and "false A" events which occurred during the real time record. Subtraction of these identified "spurious" events from the total number of events recorded permitted another table to be prepared, indicating the total number of "B" events and the total number of observed or "unhidden A" events, as well as those "hidden A" events which did not occur at the predictable times of arrival of the periodic interfering impulses. This table was constructed for all three channels for each orbit. The total time of received signal available for each portion of this tabulated information (per orbit) was also recorded. These data are presented as Tables 3 through 6.

7.4.4 Because of the peculiar nature of the data-handling equipment, which presented a real-time indication only of every other "A" event, an ambiguity exists at the beginning and end of each segment of data in which there is a possibility one of the "hidden A" events may have occurred. It should be noted in this connection that no such ambiguity exists in the central portion of each record. The fact that a level switch has occurred provides exact information as to whether an "even" or "odd" "A" event has just transpired, when compared to the preceding and succeeding transitions in the level of the telemetry signal. For this reason, a second entry was made in the table indicating the total number of seconds of data time at the leading and trailing edges of each burst of data per orbit, where this possible ambiguity of unobservable events might have occurred. The method chosen as most valid for analysis of these data was exclusion of these ambiguous portions of the total record from each individual pass, and consideration of either the first or the last observed event as a "clearing" or "reset" pulse. Essentially identical results are achieved for the total amount of information on each channel, regardless of whether the first event is not counted but regarded as a "reset" impulse and all observed

52

TABLE 3

Tabulated Record Readout Time in Seconds from 1961α1

Available for Analysis by Orbit and Station

Orbit	Station	System Recording Time	Total Sample Time/orbit	Channel 38		Channel 40		Channel 42	
				Events Ambiguous	Events Not Ambiguous	Events Ambiguous	Events Not Ambiguous	Events Ambiguous	Events Not Ambiguous
1	K	78623-79033	1211 sec	698 sec	513 sec	1211 sec	0 sec	1211 sec	0 sec
1	V	78996-79433							
1	H	79254-79834							
2	K	84760-84927	659	302	357	145	514	24	635
2	H	84880-85419	287	219	68	65	222	36	251
5*	N.B.	14019-14306	269	187	82	75	194	25	244
6*	N.B.	19736-20005	666	110	556	300	366	26	640
7	V	25072-25738	663	208	455	156	507	30	633
8	V	30696-31359	38.5	38.5	0	38.5	0	38.5	0
9	K	37101.5-37140	330	208	122	208	122	28	302
13*	N.B.	61123-61453	132	132	0	132	0	40	92
14	N.B.	66704-66735	507	256	251	140	367	50	457
	N.B.	66879-66980	784	784	0	28	756	28	756
15*	V	72430-72937	644	644	0	100	544	40	604
16*	V	78048-78572	542	95	447	305	237	28	514
16*	P	78336-78832	327	210	117	103	224	6	321
17	H	83949-84593							
22	V	24256-24798							
23	V	29772-30099							
Total Times (seconds)			5848.5	3393.5	2455	1755.5	4053	399.5	5449

Note I. Times indicated for Orbit 1 not included in totals.

Note II. Orbits which are gap filled are indicated by asterik (*).

53

TABLE 4

Channel 38 Data Readout

Serial No. 4, Lateral   A threshold = 0.55 mgm cm/sec
A_h = hidden A   B threshold = 4.00 mgm cm/sec

Orbit	Unambiguous Total Events			Ambiguous Events	Spurious Events			Net Unambiguous Events		
	B	A	A_h	A_h	B	A	A_h	B	A	A_h
2	1	2	2	2	0	0	0	1	2	2
5	0	2	1	2	0	0	0	0	2	1
6	0	3	2	2	0	0	0	0	3	2
7	2	6	7	2	0	1	1	2	5	6
8	1	4	4	2	1	0	0	0	4	4
9	0	0	0	1	0	0	0	0	0	0
13	0	2	1	2	0	2	1	0	0	0
14	0	0	0	2	0	0	0	0	0	0
15	2	1	1	2	0	0	0	2	1	1
16	1	0	0	2	0	0	0	1	0	0
17	0	1	0	2	0	0	0	0	1	0
22	4	5	4	2	0	0	0	4	5	4
23	0	2	1	2	0	0	0	0	2	1
Total	11	28	23	25	1	3	2	10	25	21

Max. Total for System   (A+B) events   B events
                                  81   10

Min. Total for System   56   10

Unambiguous Total (excluding clearing pulses)   47-48   8

TABLE 5

Channel 40 Data Readout

Serial No. 5, Lateral   A threshold = 0.28 mgm cm/sec
                         B threshold = 4.00 mgm cm/sec

Orbit	Unambiguous Total Events			Ambiguous Events	Spurious Events			Net Unambiguous Events		
	B	A	Ah	Ah	B	A	Ah	B	A	Ah
2	0	6	5	2	0	6	5	0	0	0
5	0	3	2	2	0	3	2	0	0	0
6	0	2	1	2	0	2	1	0	0	0
7	1	3	3	2	0	3	2	1	0	1
8	1	4	4	2	0	1	1	1	3	3
9	0	0	0	1	0	0	0	0	0	0
13	0	3	2	2	0	3	2	0	0	0
14	0	1	0	3	0	1	0	0	0	0
15	0	7	6	2	0	6	4	0	1	2
16	0	11	9	1	0	9	8	0	2	1
17	0	6	5	2	0	6	5	0	0	0
22	1	6	6	2	0	1	1	1	5	5
23	0	4	3	2	0	2	2	0	2	1
Total	3	56	46	25	0	43	33	3	13	13

Max. Total for System   (A+B) events   54   B events   3

Min. Total for System   29   3

Unambiguous Total (excluding clearing pulses)   25-27   2-3

55

TABLE 6

Channel 42 Data Readout

Serial No. 8, Aft   A threshold = 1.06 mgm cm/sec
                     B threshold = 3.09 mgm cm/sec

Orbit	Unambiguous Total Events			Ambiguous Events	Spurious Events			Net Unambiguous Events		
	B	A	Ah	Ah	B	A	Ah	B	A	Ah
2	5	10	10	2	5	9	8	0	1	2
5	5	5	5	2	5	5	1	2	0	4
6	10	2	1	2	8	1	0	2	1	1
7	11	7	7	2	8	7	7	3	0	0
8	11	7	9	2	8	6	8	3	1	1
9	1	0	0	2	1	0	0	0	0	0
13	3	4	4	2	3	4	4	0	0	0
14	1	2	1	3	1	2	1	0	0	0
15	10	1	6	2	10	1	5	0	0	1
16	16	6	9	2	13	6	6	3	0	3
17	12	9	3	2	11	7	3	1	2	0
22	14	8	5	1	10	5	3	4	3	2
23	9	5	10	1	5	3	3	4	2	7
Total	108	66	70	25	86	56	49	22	10	21

Max. Total for System   (A+B) events   B events
                            78   22

Min. Total for System   53   22

Unambiguous Total (excluding clearing pulses)   52   21-22

succeeding events tabulated, or the first event is counted and the last event is not counted, but considered as the "clearing" pulse which restores all registers to a known position and thus terminates an individual segment of the record.

7.4.5 In order to complete the analysis, it is necessary only to correct the total number of events for the effective area of the collecting surface. Simple computation from the physical dimensions of sensor assembly C12DM01B indicates a total effective area of .0504 square meters per system. Use of this area, together with the tabulated number of real time events which occur within the total time and are not definitely ascribable to the repetitive interfering signal, permits computation of two ("A" and "B") values per system. These represent final influx rates for the two momentum thresholds calibrated for each system.

7.4.6 In order to explore the total range of threshold momenta versus influx rate computations which might be obtained from different interpretations of the same raw data, computations were also made based upon the total number of events definitely noted in the unambiguous portion of the record, and upon the total possible number of "hidden A" counts considered over the total time of exposure per orbital record for the entire vehicle. These are represented as a maximum interpretation. A similar minimum interpretation can be achieved by assuming none of the ambiguous "hidden A" events at the beginning or end of each portion of the record were actually stored, and computing influx rates based only upon those unambiguous events in the central portion as the total for the entire time of exposure of each system. These represent the extremes within which computed influx rate must necessarily lie.

7.5 For comparison purposes, influx rates based upon the data recorded from early rocket experiments have been computed with similar assumptions.

7.5.1 After consideration of the various factors surrounding each of the early rocket experiments, four were selected as having the greatest probability of valid data. Nike-Cajun rounds AA6.203 and AA6.204 appear well calibrated and well document 1, although some periodic interference can be noted in the records. Spaerobee AA10.01 and Aerobee 88 (skin system only) also appear to have been reasonably successful; analysis was restricted to these four rounds. Calibration thresholds and total number of events were obtained from the final report on AF 19(604)-1908. (Ref. 1)

7.5.2 A considerable range of influx rates can be computed, depending upon the assumptions adopted. Maximum interpretation is possible by counting both definitely confirmed and questionable (but not showing definite negative correlation) events tabulated in the final report. Minimum influx figures in this instance represent only those pulses which show definite correlation, or for which no suspicion of internal interference exists in the explanatory notes in the above-mentioned final report.

Because there had been earlier speculation that many
of the events in the early rocket flights were obtained due to thermal
mechanism in which the aerodynamic heating effect created extraneous
mechanical disturbances which were coupled to the acoustic detection
devices, the rocket data have also been considered only for that portion
of the flight which occurred after zenith and above 100 kilometers alti-
tude. In general, slightly lower influx rates are achieved by this
method of analysis. These rates might be classed as of greater validity,
except that both the total number of events and time of exposure avail-
able for analysis are seriously limited by this approach.

7.6 The results obtained in the influx rate evaluation for both
rocket and satellite data may be combined in a single analysis.

7.6.1 The most probable interpretation of influx rates from
the 1961α1 vehicle are shown in Figure 22 ⊢ the heavy solid lines. As
will be noted, excellent agreement with a straight line fit exists for
data from both Serial Number 8 and Serial Number 4 systems. The data
from Serial Number 5 yields influx rates approximately one order of
magnitude less than those indicated by Serial Numbers 4 and 8. All
three systems show a relatively constant slope of influx rate versus
sensitivity when comparing the lesser "A" threshold with the larger "B"
threshold. A unity slope would represent a simple inverse relationship
between number of particles and momenta of the particles, i.e., directly
proportional and higher number of particles possessing the lower momentum
values. This is consistent with some early theories regarding mass
distribution effects. Most probable influx rates, together with the
ranges possible for alternate interpretations, follow as Table 7.

MICROMETEORITE INFLUX RATES

Table 7 - 1961α1

System	Threshold Momentum (Mgm cm/sec)	Influx Rate (No/Meter^2/Sec.)		
		Most Probable	Maximum	Minimum
D12DN01B				
S/N 4	0.55	0.387	0.456	0.190
S/N 4	4.00	0.065	0.081	0.034
S/N 5	0.28	0.127	0.183	0.092
S/N 5	4.00	0.012	0.015	0.011
S/N 8	1.06	0.190	0.265	0.180
S/N 8	3.09	0.079	0.021	0.075

7.6.2 Influx rates computed from the early rocket data dis-
close that the same general region is embraced by both rocket and
satellite information. For ready comparison, the rates from these
sources are also plotted on Figure 22. The actual maximum and minimum
rates calculated for data above 100 kilometers follow as Tables 8 and 9.
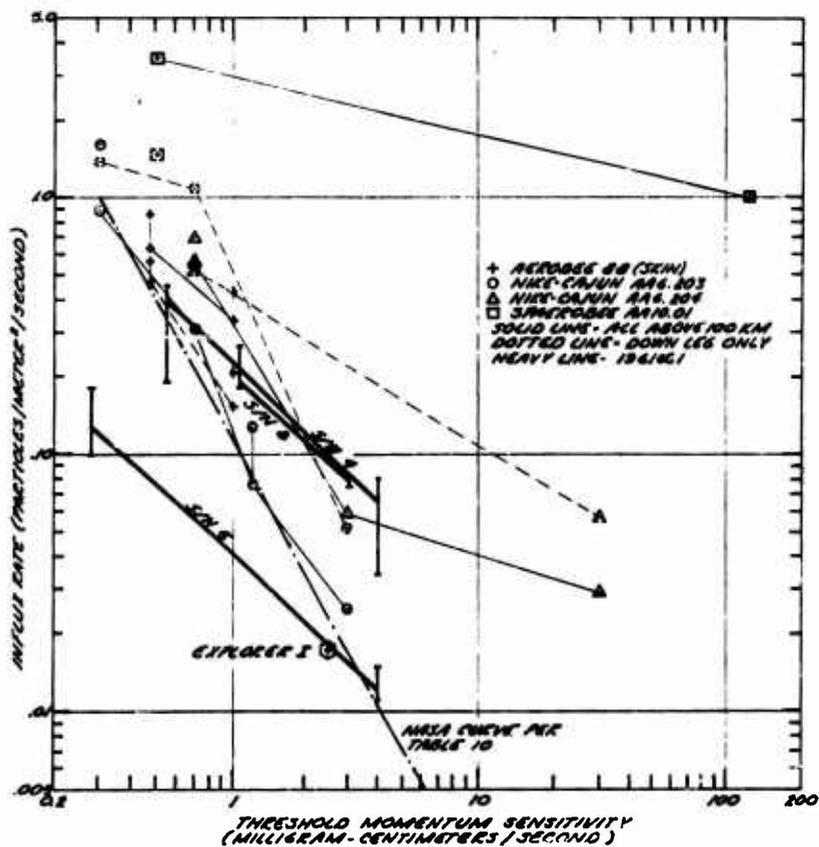
Figure 22. Micrometecrite Influx Curves

Table 8

OSU Rocket Data (Entire Flight Above 100 KM Altitude)

System	Threshold (Mgm cm/sec)	Max. No.	Maximum Influx Rate (No/M^2/sec)	Min. No.	Minimum Influx Rate (No/M^2/sec)
Aerobee 88 (skin)	0.47	34	0.855	25	0.630
Aerobee 88 (79 sec)	1.00	17	0.427	13	0.327
AA6.203 (197 sec)	0.30	63	1.600	35	0.889
AA6.203 (197 sec)	0.70	26	0.661	12	0.305
AA6.203 (197 sec)	1.20	5	0.127	3	0.076
AA6.203 (197 sec)	3.00	1	0.025	1	0.025
AA6.204 (172 sec)	0.70	24	0.697	19	0.552
AA6.204 (172 sec)	3.00	2	0.058	2	0.058
AA6.204 (172 sec)	30.00	1	0.029	1	0.029
AA10.01 (205 sec)	0.50	29	3.450	--	-----
AA10.01 (205 sec)	120.00	1	1.000	--	-----

Table 9

OSU Rocket Data (Downleg from Zenith to 100 KM Altitude)

System	Threshold (Mgm cm/sec)	Max. No.	Maximum Influx Rate (No/M^2/sec)	Min. No.	Minimum Influx Rate (No/M^2/sec)
Aerobee 88 (skin)	0.47	11	0.565	9	0.461
Aerobee 88 (39 sec)	1.00	4	0.205	3	0.154
AA6.203 (97 sec)	0.30	27	1.390	27	1.390
AA6.203 (97 sec)	0.70	21	1.081	21	1.081
AA6.203 (97 sec)	3.00	1	0.052	1	0.052
AA6.204 (87 sec)	0.70	10	0.574	9	0.518
AA6.204 (87 sec)	30.00	1	0.057	1	0.057
AA10.01 (120 sec)	0.5	7	1.458	--	-----

7.6.3 Recent information from McCracken of N.A.S.A. (Ref. 5) is also of interest for comparison purposes. Although data are customarily presented at N.A.S.A. in terms of influx rate versus particle mass, the assumption of a mean velocity of 30 kilometers per second for all particles will permit presentation on the momentum basis used in Figure 22. A smooth curve approximately fitting all available data is given in Table 10, together with approximate influx rate and momentum thresholds for a number of satellite experiments other than 1961ω1. The general curve is also shown on Figure 22 over the momentum range herein discussed. A weighted mean value for sounding rocket composite data is also quoted and appears reasonably consistent with the new evaluation at the high sensitivity end (ref. AA6.203 influx rate range at 0.3 mgm cm/sec).

Table 10

N.A.S.A. Data (McCracken, 25 October 1961)

Log_{10} Influx (No/M^2/sec) $\cong$ -17.0 - 1.70 log_{10} mass (grams)

System	Threshold (Mgm cm/sec)	Exposure (M^2 sec)	Influx (No/M^2sec)
Explorer I	2.5	1.8×10^4	0.037
Pioneer I	0.15	4.2×10^3	0.0043
Vanguard III	10.00	2.4×10^6	0.002
Explorer VIII	3.00	---------	0.02
Explorer VIII	30.00	---------	0.0004
Explorer VIII	300.00	---------	0.000008
Rocket Composite	0.30	---------	1.00

7.6.4 In view of the above discussion, it would appear that there is no reason for excluding or considering irreconcilable micrometeorite influx data achieved from early rocket experimentations to which reasonable weight can be ascribed and the rates determined through more recent investigations by means of satellite vehicles.

7.7 A discussion of the data and results achieved in the analysis may now be in order.

7.7.1 Several specific details of possible significance became evident during the study of both the original strip charts and the master chart prepared from them.

7.7.1.1 A severe level compression and shift to DC output levels above the original settings, accompanied by a differentiation of the step function representing each level change, was evident on the channel 38 signal. The distortion was uniform throughout the flight at all receiving stations. It was particularly evident during the overlap period in Orbit 1, when the Vandenberg record showed six of the eight possible levels approximately 0.3 volts above the simultaneous record obtained at the Hula station.

7.7.1.2 The first 455 seconds of record during Orbit 1 show all channels at the calibration level of +5.0 volts, an impossible condition in view of the fact that the maximum logic level ranged from 4.1 to 4.6 volts for the systems involved over the entire flight. The next 804 seconds of data from Orbit 1 showed nothing on channel 40, the most sensitive system, and a single B event (probably spurious) on channel 42, but 20 "A" and 3 "B" events on channel 38 within a 413 second period. This is several times the rate indicated for any following information. (Data from Orbit 1 are excluded from the analysis; it is speculated that vehicle aspect was stabilized during this period).

7.7.1.3 The three-point pre-calibration and five-point post-calibration frequently differ by 10 per cent from one another on a single playback record. The choice of 0.6 volt increments for an

61

eight-level output indication was wise, as 0.3 volt increments would be ambiguous unless certain groups occurred within a given chart.

7.7.2 Calibration of the threshold momentum sensitivities for all three systems flown was performed several months prior to launch, and was accomplished by the early technique in which glass spheres of known mass were dropped from calibrated heights to establish the threshold limits. This technique was not repeatable, nor as reliable as the electronic striker technique developed later.

7.7.2.1 It is possible that the discrepancy in influx rates deduced from Serial Number 5 data resulted from a decrease in amplifier sensitivity, which would have displaced both points to the left in Figure 22, so far as momentum thresholds are concerned. If compensation for this effect could be accomplished, it would bring them into closer agreement with that influx information deduced from Serial Numbers 4 and 8.

7.7.2.2 It is also possible that the prolonged time period between initial calibration and final flight installation encompassed some damage to the systems. It should be mentioned that early verbal reports indicated that the sensor system associated with system Serial Number 8 was mechanically damaged prior to actual launch of this experiment and that the sensor assembly was deformed to the point where mechanical contact was possible between the normally isolated sensor plate and the mechanical structure supporting the entire assembly. This would have rendered Serial Number 8 extremely sensitive to pickup of extraneous interference due to such things as closure of relays or operation of mechanical equipment located elsewhere in the payload. A study of the tabulated data discloses that a total of 191 spurious events, spaced at 30-second intervals, were noted on this particular channel 42 record. The channel 40 record for Serial Number 4 had a higher threshold sensitivity than either the system on channel 38 or 42. However, the structure was apparently not damaged in this instance. A total of 76 events exhibiting a time coincidence with the spurious pulses described as appearing on channel 42 were observed on channel 40, whereas a total of only four or six such spurious events were noted on the less sensitive system telemetered on channel 38. A single triple coincidence occurred during the useful portion of the record. This event occurred on Orbit 13 on the New Boston record.

7.7.3 A total of 5,848.5 seconds of recorded signal were available (exclusive of Orbit 1). Some gaps have been filled in instances where no ambiguous count resulted; i.e., in those cases where there was no real time event or where the real time events which might have occurred during loss of synchronization were such that the data register advanced unambiguously to the next possible logical indication. This total time includes filling of such gaps on various orbits. Orbits in which "gap fill" was used to extend the total data sampling time are noted in Table 3.

7.7.4 The one-per-second sampling rate inherent in the commutated data transmission system employed has made exact time-coincidence indeterminable for the postulated 30-second periodicity of

spurious signals. A time resolution of only one second is possible when comparing channel 38 and channel 40 events with those definitely spurious events noted on channel 42. This means that some real data pulses may have been discarded as spurious simply because they occurred during the same one-second interval as was occupied by a spurious pulse on channel 42. This effect would tend to depress the influx rate for Serial Number 5, which was tabulated as indicating 76 spurious events and only 29 real events after cross-correlation for time-coincidence with the channel 38 signal.

7.7.5 A single illogical sequence was noted in the 339 transitions available for study in the composite record. This sequence occurred near the end of the channel 42 Hula record for Orbit 17, and may represent a malfunction of the logic circuitry. However, it is more probable that three events occurred in close juxtaposition, causing the one-per-second decommutation rate to omit one level from the sequence.

7.7.6 A single displaced bar in the decommutated channel 40 record from Vandenberg for Orbit 22 was judged a loss of synchronization. It could also represent a pair of closely spaced B events without violating the logical sequence possible. This alternate interpretation would raise the most probable influx rate for 4.0 mgm cm/sec on Serial Number 5 from .012 to .022 particles per square meter per second.

7.8 Results of the data analysis may be summarized as follows:

The best interpretation possible from the records of telemetered information from 1961σ1 discloses that the computed micrometeorite influx rates for the observed range of momenta do not differ substantially from those achieved in earlier rocket and satellite instrumentation. For both satellite and rocket data, approximately one order of magnitude separated minimum from maximum influx rates obtained by different systems and under various assumptions of analysis. For any one given system, a reasonable relationship between two respective momentum thresholds is clearly observable, and the influx figures appear to verify an earlier mass distribution function of constant mass per unit volume, regardless of particle size. However, the limited number of events available for analysis in the present study and the relatively disproportionate number of spurious events relative to real events must of necessity cast some doubt upon the interpretations reported herein. A representative mean influx rate for particles possessing a momentum of one mgm cm/sec is of the order of 0.1 particle/square meter/second, with an uncertainty of a factor of $\pm$ 2:1.

8.0 SUMMARY AND CONCLUSIONS

8.1 The primary objective of Contract AF 19(604)-5715 was to sponsor the design, development, and construction of micrometeorite detection systems employing the acoustic technique for use on satellites.

The research and development phase, which is essential to the design of high quality equipment, was continued throughout the major portion of the contracting time. This extended endeavor was predicated

63

by the hardware delivery schedule and the time duration of the contract. The amplifier design, which was used in Model D14DN01 systems, could not be finalized during the short period of time between initial effort and scheduled delivery. As a result, an amplifier with proven reliability, but with reduced sensitivity, was incorporated in the Model D12DN01B systems to fulfill delivery requirements, while the new improved amplifier was undergoing acceptance testing. Improvements in the DC to DC power converter were made possible by the acquisition of a toroid winding machine and new developments in the field of tape wound cores, which were introduced as commercial items subsequent to the initial design of the converter. These are typical examples of the continued efforts to achieve design improvements, which were conducted concurrently with production obligations.

8.2   Since the micrometeorite detection systems were to be installed on satellites and information regarding the available power was not explicit, early coordination suggested that the detection system should be designed for absolute minimum power consumption. This criteria was followed throughout the design crd production of all systems constructed under this contract. The overall effect of the minimum power design cannot be evaluated by an empirical method, but the leakage current problems discussed in Section 5 could have been alleviated if the biasing current for the transistors had been of greater magnitude.

8.3   Germanium transistors were used throughout the detection system. At the time of preliminary design and later production of the systems, the additional cost of silicon transistors was prohibitive. Another unattractive feature inherent with silicon transistors, at that time, was the low base-to-emitter breakdown voltage. The transistors could have been protected by installing diodes in the emitter circuits, but this would have increased production costs to higher extremes. System reliability could have been improved by converting to the silicon transistor regardless of costs and allowing a more liberal bias current.

As a result of continued advancements in the field of semiconductor technology and increased application, improved silicon transistors are now available commercially at price levels lower than the original cost of the germanium transistors employed in the micrometeorite detection systems. Silicon semiconductors are recommended for future hardware that is subject to extreme fluctuations in ambient temperatures.

8.4   The information which was presented in Section 7 pointed out the difficulties encountered with the "hidden A" storage facility in the logic of the micrometeorite detection system. If telemetry records had been available for analysis during the earlier stages of this program, this problem would have been recognized. After the data reduction had been accomplished, a recommendation was made that all remaining systems should be converted to an "all event" presentation. Several systems were returned for modification as a result of this recommendation. Two options were possible: the jumper connection could be so made as to present a total of 16 discrete data levels, eight in the upper half and eight in the lower half. This would leave unchanged the total

64

storage register capacity of eight A events before recycle. If telemetry channel noise considerations are such as to make ambiguous the resolution of 16 discrete levels, (note that 16 logic levels implies only 0.3 volt difference in output signal per level, a possible ambiguous condition mentioned previously) the alternate configuration should be used in which total storage capacity is only four events at the lower "A" momentum threshold before recycling. In any event, elimination of the "hidden" event in the data readout philosophy would improve the validity of information obtained from future experiments.

8.5 Another conclusion, based on the data analysis in Section 7, is that more elaborate equipment checkout procedures should be instituted prior to launch of vehicles carrying micrometeorite detection systems. The periodic interference noted on records from 1961α1 should have manifested itself in the prelaunch check activities as a characteristic repeatable signal, evident twice per minute on one channel of the telemetry, and measures could have been taken to identify the component of the payload generating this interference.

8.6 Because of the discrepancy noted in records from 1961α1 between information from Serial Number 5 as compared to that obtained from Serial Numbers 4 and 8, additional and more sophisticated checks of threshold momentum sensitivity should be made as closely as possible to actual launch time. As a further refinement to future systems, it is suggested that some modification of the electronic striker technique be employed for actual inflight calibration of the systems.

8.7 Inclusion in the telemetered data of the previously provided but unused internal temperature monitor would facilitate analysis of possible shifts in momentum thresholds or other possible malfunctions such as the distortion and output level compression noted in data from Serial Number 4. This also provides valuable design information for future system development.

65

REFERENCES

1. Buck, R. F., "Acoustic Detection of Meteoric Particles," Oklahoma State University, Research Foundation, Final Report on Contract AF 19(604)-1908, AFCRC-TR-60-272, April 14, 1960.

2. Buck, R. F., "Development of Apparatus for Micrometeorite Measurements," Oklahoma State University, Research Foundation, Final Report on Contract AF 19(604)-7202, Project No. P7667, Task No. T76046, December 1961.

3. Mueller, D. C., "A Transistorized Digital Computer with Both Real and Stored Time Analog Readout of Information—For Use in Deep Space Investigations of Micrometeor Phenomena," M. S. Thesis, Oklahoma State University, August 1960. Included under separate cover as Appendix I to this report on Contract AF 19(604)-5715.

4. Mueller, D. C., "Interim Engineering Report on System D14DN01," Oklahoma State University, Research Foundation, Appendix to Quarterly Status Report No. 4 on Contract AF 19(604)-5715, 1 March 1960 through 31 May 1960.

5. McCracken, C. W. and Alexander, W. M., "The Distribution of Small Interplanetary Dust Particles in the Vicinity of the Earth," N.A.S.A. TN D-1349, Goddard Space Flight Center, July 1962.

6. "Research Directed Toward the Design, Development and Construction of Meteoric Microphone Detectors of Various Sensitivities for Use in Satellites," Oklahoma State University, Research Foundation, Scientific Report No. 1 on Contract AF 19(604)-5715, AFCRC-TN-60-229, January 1960.

7. Soberman, R. K. and Della Lucca, L., "Micrometeorite Measurements From the Midas II Satellite (1960ξ1)," AFCRL, GRD Research Notes No. 72, November 1961.